Cosmogenic exposure dating in arctic glacial landscapes: implications for the glacial history of northeastern Baffin Island, Arctic Canada

Jason P. Briner, Gifford H. Miller, P. Thompson Davis, and Robert C. Finkel

Abstract: Cosmogenic exposure dating and detailed glacial-terrain mapping from the Clyde Foreland, Baffin Island, Arctic Canada, reveal new information about the extent and dynamics of the northeastern sector of the Laurentide Ice Sheet (LIS) during the last glacial maximum (LGM). The Clyde Foreland is composed of two distinct landscape zones: (1) glacially scoured terrain proximal to the major sources of Laurentide ice that flowed onto the foreland, and (2) ice distal unscoured sectors of the foreland. Both zones are draped with erratics and dissected by meltwater channels, indicating past ice cover. We interpret the two landscape classes in terms of ice sheet erosive ability linked with basal thermal regime: glacially scoured terrain was occupied by erosive warm-based ice, and unscoured terrain was last occupied by non-erosive cold-based ice. Cosmogenic exposure ages from >100 erratics from the two landscape types have different age distributions. Cosmogenic exposure ages from the glacially scoured areas suggest ice cover during the LGM, followed by deglaciation between ~15 and ~12 ka. In the unscoured lowlands, the cosmogenic exposure ages have multiple modes ranging between ~12 and ~50 ka, suggesting multiple periods of cold-based ice cover during the last glacial cycle. In landscapes covered by cold-based ice, large numbers of cosmogenic exposure ages are required for elucidating glacial histories.

Résumé : La détermination des âges d'exposition aux rayonnements cosmogéniques et une cartographie détaillée du terrain glaciaire de l'avant-pays Clyde, île de Baffin, dans l'Arctique canadien, révèlent de nouvelles informations sur l'étendue et la dynamique du secteur nord-est de l'inlandsis laurentidien au cours du dernier maximum glaciaire. L'avant-pays Clyde présente deux zones à paysages distincts : (1) un terrain affouillé par les glaciers à proximité des sources majeures de la glace laurentidienne qui s'écoulait vers l'avant-pays et (2) les secteurs de l'avant pays non affouillés par la glace distale. Les deux zones sont recouvertes de blocs erratiques et découpées par des chenaux d'eau de fonte, indiquant une couverture glaciaire antérieure. Nous interprétons les deux classes de paysages en termes de capacité d'érosion de la couche glaciaire reliée au régime thermique de base : le terrain affouillé par la glace était recouvert par de la glace érosive, à base tempérée, et le terrain non affouillé était recouvert par de la glace non érosive à base froide. Les âges d'exposition aux rayonnements cosmogéniques de plus de 100 erratiques provenant des deux types de paysages ont des distributions d'âges différentes. Les âges d'exposition aux rayonnements cosmogéniques des endroits affouillés par la glace suggèrent une couverture glaciaire durant le dernier maximum glaciaire, suivie d'une déglaciation entre ~15 et ~12 ka. Dans les basses terres non affouillées, les âges d'exposition aux rayonnements cosmogéniques ont des modes multiples allant de ~12 à ~50 ka, suggérant de multiples périodes à couvert de glace à base froide durant le dernier cycle glaciaire. Dans les paysages recouverts par de la glace à base froide, beaucoup d'âges d'exposition aux rayonnements cosmogéniques sont requis afin d'établir les historiques glaciaires.

[Traduit par la Rédaction]

Introduction

Precise and accurate chronologies for alpine-glacier and ice-sheet fluctuations are crucial for understanding the Quaternary ice age, glacier processes, and spatial patterns of global climate change. Over the past decade, cosmogenic exposure (CE) dating has provided dozens of late Pleistocene glacial chronologies from regions spanning the globe, including both alpine (e.g., Gosse et al. 1995; Phillips et al. 1997; Owen et al. 2002) and continental ice-sheet settings (e.g., Swanson and Caffee 2001; Balco et al. 2002). However, similar to other geochronological tools, a rigorous set

Received 15 December 2003. Accepted 22 November 2004. Published on the NRC Research Press Web site at http://cjes.nrc.ca on 7 February 2005.

Paper handled by Associate Editor R. Gilbert.

J.P. Briner[1, 2] and G.H. Miller. INSTAAR and Dept. of Geological Sciences, University of Colorado, Boulder, CO 80303, USA.
P.T. Davis. Dept. of Natural Sciences, Bentley College, Waltham, MA 02454, USA.
R.C. Finkel. Center for Accelerator Mass Spectrometry, Lawrence Livermore National Laboratory, Livermore, CA 94550, USA.

[1]Corresponding author (e-mail: jbriner@buffalo.edu).
[2]Present address: Department of Geology, 876 Natural Sciences Complex, University at Buffalo, Buffalo, NY 14260, USA.

 doi: 10.1139/E04-102

Fig. 1. (A) The eastern Canadian Arctic showing Baffin Island and the extent of the Laurentide Ice Sheet (LIS) during the last glacial maximum (from Dyke et al. 2002). Inset shows the LIS on North America. (B) Fiords and coastal lowlands of northeastern Baffin Island. Thin dashed line represents the early Holocene extent of the LIS; thick dashed line approximates the current LGM reconstruction from Dyke et al. (2002). Topography from 90-m grid-cell resolution Canadian digital elevation data, and off-shore bathymetry from Løken and Hodgson (1971). Location shown in Fig. 1A.

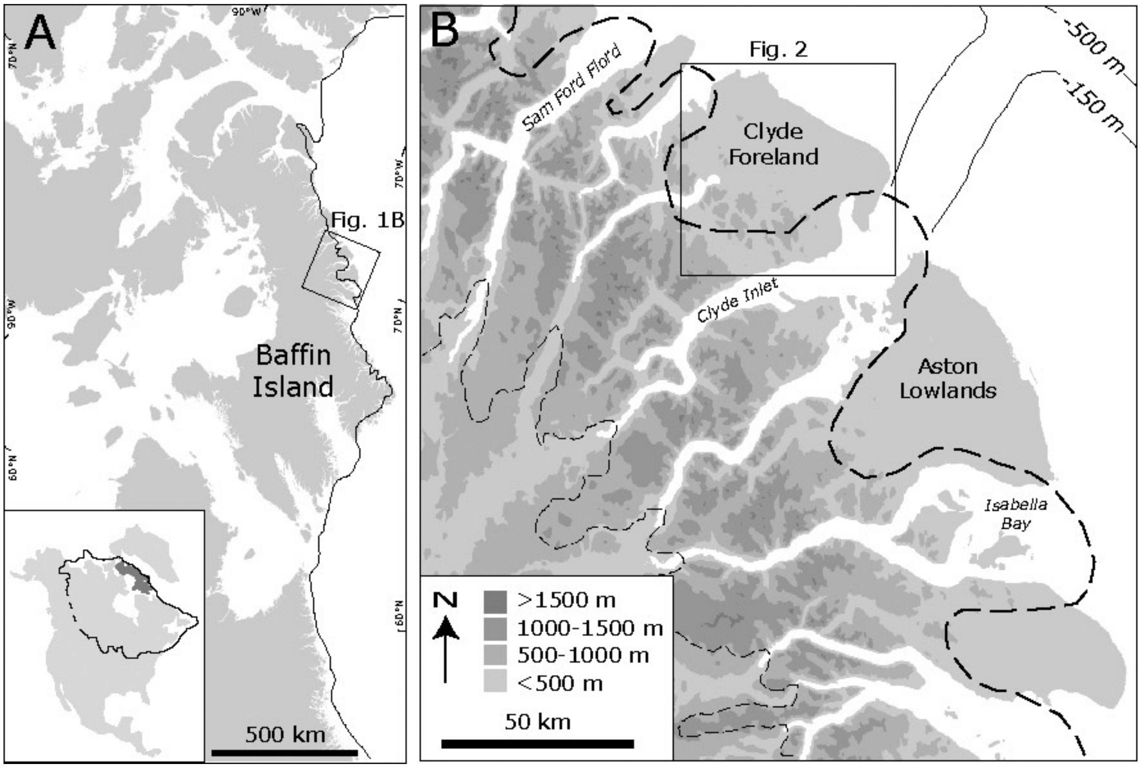

of guidelines is necessary to establish a robust glacial chronology using CE dating (e.g., Gosse and Phillips 2001). The majority of CE dating has been carried out in non-polar latitudes, where glaciers are typically warm-based (i.e., glaciers slide across and erode their beds).

The Arctic is one of the most heavily glaciated regions on the planet, but CE dating studies in arctic areas aiming to establish glacial chronology can be complicated (e.g., Marsella et al. 2000; Miller et al. 2002; Kaplan and Miller 2003). Obtaining precise chronologies from arctic areas is important because comparing chronologies from northern ice-sheet margins to those of their southern margins helps to elucidate Northern Hemisphere ice-sheet response to climate change (e.g., Miller and deVernal 1992; Svendsen et al. 1999). Although CE dating holds promise for establishing detailed chronologies in polar areas, account must be taken of the difference in basal ice-sheet processes that are dominant in the Arctic compared with those at lower latitudes. Efficient glacial erosion is an important assumption for CE dating studies but may be hampered where ice sheets are cold-based. The validity of the efficient glacial erosion assumption must be considered when applying CE dating in arctic glacial landscapes.

Here, we present CE ages from 103 glacial erratics from the Clyde Foreland on northeastern Baffin Island (Fig. 1), situated along the coastal margin of the northeastern sector of the former Laurentide Ice Sheet (LIS). While aiming to constrain better the Late Pleistocene glacial history of northeastern Baffin Island, we determined that CE dating in this region is complex because of locally inefficient ice-sheet erosion. Here, we explore the use of CE dating in arctic glacial landscapes, where ice sheets were partly cold-based and non-erosive, and discuss the implications of the CE ages for the history of the northeastern sector of the LIS.

Background and setting

Glacial history of the eastern Canadian Arctic

Reconstructions of the LIS have differed widely over the past century. Ice margin reconstructions for the Last Glacial Maximum (LGM) have remained approximately the same along the southern margin of the LIS, but reconstructions along the eastern Canadian seaboard have ranged from ice terminating at the continental shelf break (e.g., Flint 1943; Hughes et al. 1977; Denton and Hughes 1981; Jennings et al. 1996; Hughes 1998), to ice terminating hundreds of kilometres inland at the heads of fiords and sounds (Coleman 1920; Miller and Dyke 1974; Andrews 1987; Dyke and Prest 1987). The most recent LIS reconstruction shows the ice margin in an intermediate position near the mouths of fiords and sounds (e.g., Jennings et al. 1996; Dyke et al. 2002; Miller et al. 2002). LIS reconstructions have been most uncertain in the eastern Canadian Arctic, from Labrador to the Canadian High Arctic archipelago (Fig. 1), because of a dearth of datable materials that can be directly linked with glacial deposits.

Fig. 2. Physiography of the Clyde Foreland. Topography from 90-m grid-cell resolution Canadian digital elevation data. Location shown in Fig. 1.

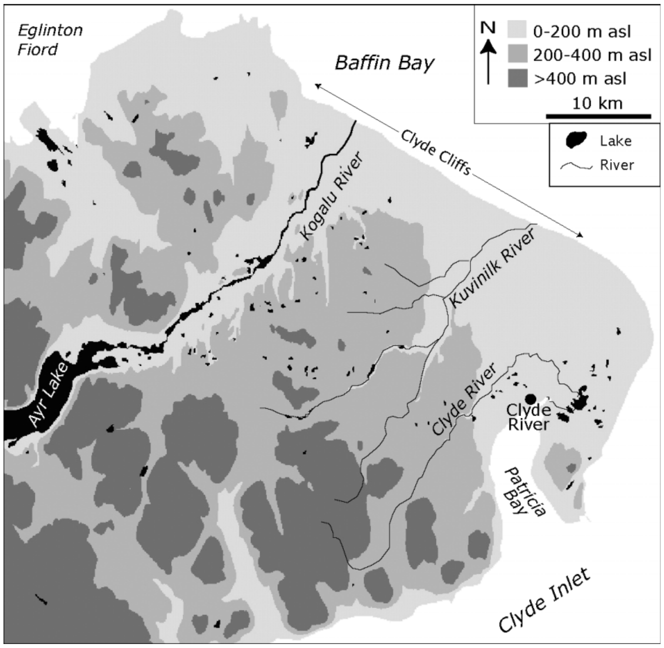

Fig. 3. Ice limit map of the Clyde Foreland. Rivers and lakes (Fig. 2) have been removed for clarity. Mapped ice margins defined by moraines and meltwater channels. Black arrows represent ice flow.

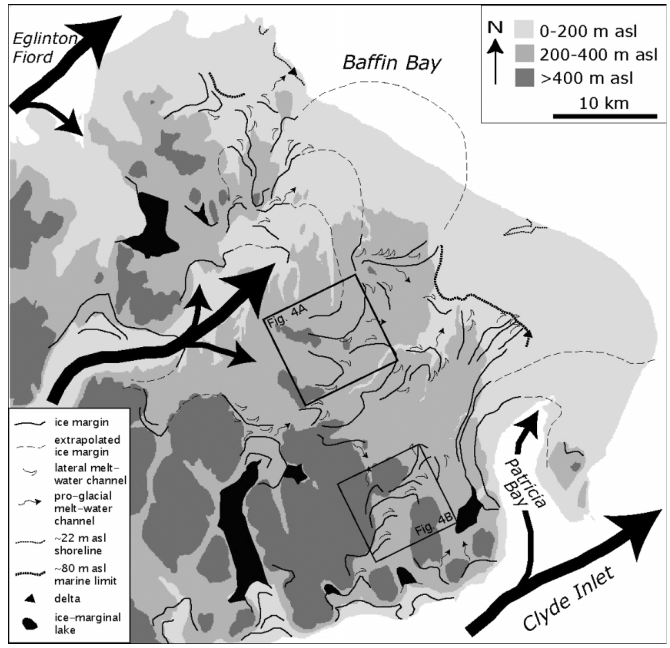

To test the Flint (1943) paradigm of a large monolithic ice dome centered over Hudson Bay and terminating on the continental shelf break, numerous researchers of the Geographical Branch of Canada visited northeastern Baffin Island in the 1960s. Rather than a simple pattern of deglaciation, they found unmodified raised marine deposits in sea-cliff exposures that were beyond the range of radiocarbon dating (>54 ka; Smith 1965; Løken 1966), coupled with highly weathered terrain that was believed to require long periods of subaerial exposure (Ives 1975). Continued work in the 1970s and 1980s supported a minimum LGM ice model (e.g., Miller et al. 1977; Dyke 1979; Ives 1978; Dyke and Prest 1987), and in the High Arctic, LGM ice extent was thought to be similar to that of extant ice today (England 1976, 1996). Differences in the relative weathering of landscapes provided much of the evidence for glacial chronologies (e.g., Boyer and Pheasant 1974; Birkeland 1978; Locke 1979) and supported restricted LGM ice.

In recent years, new approaches and techniques have improved our understanding of the LGM in the eastern Canadian Arctic. Marine cores from Cumberland Sound, southern Baffin Island, indicate that grounded LGM ice terminated in the Labrador Sea (Jennings 1993) instead of at the head of the sound (cf. Dyke 1979). Ice-sheet modeling and CE dating support Jennings' findings (Kaplan et al. 1999, 2001; Marsella et al. 2000; Kaplan and Miller 2003). In the High Arctic, CE and radiocarbon dating have recently shown that there was a large Innuitian Ice Sheet during the LGM (Zreda et al. 1999; England 1998, 1999; Dyke 1999), vastly different from some earlier interpretations (e.g., England 1976). Lake coring and CE dating on southeastern Baffin Island led to the reconstruction of low-gradient outlet glaciers extending to fiord mouths, leaving interfiord highlands unglaciated (Steig et al. 1998; Wolfe et al. 2000; Kaplan et al. 2001; Miller et al. 2002; Kaplan and Miller 2003). Most recently, CE dating has been applied to the highly weathered interfiord uplands across the eastern Canadian Arctic, long interpreted as evidence supporting restricted LGM ice (e.g., Ives 1978; Boyer and Pheasant 1974). Cosmogenic exposure ages of fresh erratics on these highly weathered uplands indicate the presence of cold-based ice cover during the LGM (Bierman et al. 2001; Briner et al. 2003; Marquette et al. 2004).

The Clyde Foreland

The Clyde Foreland, the broad coastal plain north of the hamlet of Clyde River (Fig. 2), contains a rich record of past LIS fluctuations. The foreland spans ~20 km in the east–west direction from inland mountains to a long stretch of sea cliffs bordering Baffin Bay (the Clyde Cliffs; Feyling-Hansen 1976), and ~50 km in the north–south direction from foothills between Eglinton Fiord and the Kogalu River to Patricia Bay and the mouth of Clyde Inlet in the south (Fig 2). The foreland ranges in elevation from 20 to 40 m above sea level (asl) at the cliff tops to ~250 m asl where it rises to meet the inland foothills. The foreland is mostly flat, rolling terrain, but is punctuated by several massifs reaching up to 500 m asl (Fig 2). The LIS reached the Clyde Foreland via three routes: (1) through the Ayr Lake trough and down the Kogalu River valley, spilling directly onto the foreland, (2) from Clyde Inlet to the south, where ice flowing out of the fiord impinged on the southern part of the foreland, and (3) from Eglinton Fiord, where ice spilled southward across the northern sector of the foreland (Fig. 3).

Following Smith (1965) and Feyling-Hannsen (1976), Miller (1976) and Miller et al. (1977) mapped glacial and sea-level deposits on the Clyde Foreland. They constructed a glacial and sea-level history by combining mapping with interpretations of the glacial strata exposed in the Clyde Cliffs

(Fig. 2), which include tills bracketed by shell-bearing glacial marine units. Because the shells are older than the range of radiocarbon dating, Miller et al. (1977) used amino acid geochronology to place the uppermost two till and glacial-marine-sediment packages (Ayr till and Kogalu marine sediments and Clyde till and Kuvinilk marine sediments) into the early phase of the last glaciation (Fig. 3). These packages are above the uppermost prominent buried soil (the Cape Christian Soil), which is interpreted to represent the Last Interglaciation.

Miller et al. (1977) used several lines of reasoning to infer that the Clyde Foreland was not glaciated during the LGM. First, glacial marine deposits associated with the uppermost till (Ayr till) in the Clyde Cliffs (Kogalu marine sediments) are > 50 ka. Second, the Ayr till was associated with the moraine system on the foreland (the Ayr Lake moraines), indicating that they are also > 50 ka. Third, ice limits on the foreland were related to a marine limit at ~80 m asl, which was dated to beyond the range of radiocarbon dating (Løken 1966; Miller 1976; Miller et al. 1977; Mode 1980). Bivalves associated with the ~80 m asl marine limit have amino acid ratios similar to those in Kogalu sediments, and Miller et al. (1977) assigned the ~80 m asl marine limit and Ayr till to late Marine Isotope Stage (MIS) 5 (~80 ka).

Cosmogenic exposure dating methods

Field and laboratory methods

We used CE dating to date directly a wide variety of LIS deposits on the Clyde Foreland. Samples include moraine boulders, erratic boulders, erratic cobbles and boulders perched on larger erratic blocks, and cobbles on delta and kame surfaces. We visited the Clyde Foreland in the summers of 2000, 2001, and 2003, and in May of 2002 and 2003, near the peak in snow depth. Because many surfaces are windswept on the Clyde Foreland in May, we were able to collect erratic boulder samples and cobbles from delta and kame surfaces and to observe the sample context during peak snow cover. Samples were collected using sledge hammers and chisels. Elevations were taken by combining Global Positioning System (GPS) readings with information from 1 : 50 000-scale topographic maps with 10-m contour intervals; we consider sample elevation to be accurate to ±10 m. Where possible, quartz veins were sampled, but more commonly we sampled quartz-rich granitic and gneissic surfaces. In all cases, efforts were made to sample the uppermost horizontal surfaces, and we recorded surface geometry, sample height, potential surface erosion, and sample thickness.

Samples were prepared at the University of Colorado Cosmogenic Isotope Laboratory (Boulder, Colorado) following procedures modified from Kohl and Nishiizumi (1992) and Bierman and Caffee (2001). A subset of samples (n = 11) was prepared at the University of Vermont (Burlington, Vermont) using the same procedures. Samples were crushed and the 425–850 μm fraction was retained after sieving. Samples were then treated in acid solutions to remove clays and meteoric ^{10}Be. Quartz was purified in a heated sonication bath with dilute HF–HNO_3 after heavy-liquid mineral separation. Typically, 30–40 g of pure quartz was dissolved in batches of 10 or 11 samples, with one process blank per batch; known amounts of SPEX brand Be and Al carrier were added to each sample and the blank. After complete dissolution, samples were treated with perchloric acid to remove fluoride and passed through an anion exchange column to separate Fe and Ti. Finally, Be and Al were separated using cation exchange and Al and Be hydroxides were precipitated, dried, heated to produce oxides, and packed into targets for accelerator mass spectrometric (AMS) measurement at Lawrence Livermore National Laboratory, Livermore, California. ^{10}Be/^{9}Be and ^{26}Al/^{27}Al ratios in our process blanks average $2.5 \pm 0.2 \times 10^{-14}$ (n = 26) and $1.3 \pm 0.5 \times 10^{-14}$ (n = 9), respectively.

Model exposure ages

CE ages were calculated using ^{10}Be and ^{26}Al production rates of 5.1 and 31.1 atoms g^{-}1 year^{-1}, respectively, (Stone 2000; Gosse and Stone 2001). Site-specific production rates were corrected for elevation after Lal (1991), considering both neutrons and muons according to Stone (2000), and for sample thickness. Because these samples are from high latitude (~70°N), nuclide production rates are not influenced by time-dependent changes in the geomagnetic field. The ages reported here are not corrected for atmospheric pressure anomalies, but if the average low pressure over Baffin Bay that exists today has been a persistent feature, production rates may be underestimated by ~2% in the field area (Stone 2000).

Both ^{10}Be and ^{26}Al exposure ages were calculated for 14 samples. These independent analyses exhibited good correlation (Tables 1, 2). An uncertainty-weighted average age was used for these samples. The CE age uncertainties reported here include only AMS measurement uncertainty at one standard deviation. Assigning fixed numbers to geological sources of uncertainty (e.g., post-depositional boulder stability, isotopic inheritance, and snow cover) is difficult. However, quantifying methodological uncertainties is possible. Production rates are known to within 6% (Stone 2000; Gosse and Stone 2001). Total Be and Al measurements are estimated to be accurate to 2% and 4%, respectively. AMS uncertainties average ~4%, and uncertainties associated with elevational scaling are estimated at 5% (Gosse and Phillips 2001). Thus, the propagated total methodological uncertainty for ^{10}Be is ~9% and for ^{26}Al is ~9.5%.

Several factors make the Clyde Foreland especially well-suited for CE dating. Quartz, the target mineral for ^{26}Al and ^{10}Be exposure dating, is abundant in the Canadian Shield crystalline rocks of the Clyde region (Archean layered monzogranites, granodiorites, and tonalite gneisses, and Proterozoic banded migmatites; Jackson et al. 1984). The foreland is a rocky landscape with hundreds of large erratic boulders (up to 10 m in exposed diameter). These boulders are stable because they are large, often tabular with a wide, flat base, and lie on flat, well-drained rocky surfaces. Boulder size and shape indicate that boulders have not rolled since deposition. The hamlet of Clyde River reports a mean annual temperature of –12.4 °C and a mean annual precipitation of 226 mm (http://www.climate.weatheroffice.ec.gc.ca). Much of the landscape is coarse grained and well drained with negligible periglacial activity. By sampling erratics at the time of maximum snow depth, we have concluded that snow shielding, which would lead to erroneously young ages, is probably negligible since deglaciation. Seasonal snow cover becomes significant if snowdrifts build over a sampling site, but we avoided taking samples in gullies or small depressions where snowdrifts form. Bedrock erosion, which also leads to erroneously young ages, is slow in this region (e.g., ≤1.1 mm/thousand years; Bierman et al. 1999; Briner 2003), so we treat boulder surface erosion as negligible. For erratics with a complex exposure and burial history (see later in the text), the calculated CE ages are technically *apparent* ages based on total cosmogenic nuclide concentrations.

Glacial geology of the Clyde Foreland

Key to any interpretation of a CE chronology is detailed mapping of glacial and marine features. We updated previous maps of the glacial geology on the Clyde Foreland (Smith 1965; Miller et al. 1977; Mode 1980) by mapping ice-limit features, based upon field observations and 1 : 60 000-scale black and white air photographs, onto 1 : 50 000-scale topographic maps with 10-m contour intervals. Glacial features on the foreland include erratic boulders, meltwater channels (lateral and proglacial), moraines, ice-dammed lake shorelines, and outwash terraces (Fig. 3).

Southern Clyde Foreland and Patricia Bay

A series of moraines and inter-moraine meltwater channels dominates the landscape closest to the shores of Patricia Bay (Fig. 3). Moraine ridges parallel Patricia Bay and decrease in elevation from 400–200 m asl near Clyde Inlet to 150–80 m asl at the head of the bay at a gradient of ~20 m/km, leading to a reconstructed basal shear stress (following Paterson 1994) of ~0.5 bar (1 bar = 100 kPa). On the west and north sides of Patricia Bay, the innermost moraines are sharp-crested, bouldery ridges. The moraines deflect the Clyde River (informal name) and prevent it from flowing into Patricia Bay until the river drops below the ~80 m asl marine limit, where it turns south and west into the head of the bay (Fig. 2). Tributary valleys that drain into Patricia Bay from the west contain shoreline segments that outline glacial lakes that were dammed when ice filled Patricia Bay (Fig. 3). North of the Patricia Bay moraines, meltwater channels are the dominant glacial landform. To the west of Patricia Bay, above the numerous left-lateral moraines of the Patricia Bay lobe, hills that rise to 600 m asl topped with weathered blockfields are overlain by erratics (Fig. 3). On the Black Bluff massif, east of Patricia Bay (Fig. 3), ice-sculpted bedrock and moraines occur up to 250 m asl; the top of Black Bluff massif, at ~450 m asl, consists of weathered blockfield with scattered erratics.

The Kogalu River valley

A second major pathway for ice delivery to the Clyde Foreland was via the Kogalu River valley, where the Ayr Lake lobe flowed across the central part of the foreland (Fig. 3). Ice flowing out of the deep Ayr Lake trough spread north and south through and around several high massifs that border the Kogalu River valley (Fig. 3). Near the mouth of Ayr Lake, a series of well-expressed moraine ridges and lateral meltwater channels descend from the northern valley wall to the valley floor at a gradient of ~44 m/km, leading to a reconstructed basal shear stress of ~1.2 bars. Beyond these moraines, the Kogalu lowland is a rolling, lake-dotted landscape lacking discrete moraine ridges. Where ice terminated at higher elevations on the northern and southern valley walls, numerous, well-preserved meltwater channel systems defining dozens of past ice margins were formed. In some cases, Ayr Lake ice dammed tributary valleys creating vast glacial lakes, and, in other locations, ice overtopped local drainage divides and flowed down neighboring valleys (Fig. 3). Discrete lateral meltwater channels were created at ~250 m asl, only 3 km from the coast, indicating that ice terminated beyond the modern coast at the time of channel formation.

The Kuvinilk River valley

Where the Kuvinilk River flows across the Clyde Foreland (Fig. 2), the signs of glaciation are less distinct than to the north (Kogalu River valley) and south (Patricia Bay lowland). When this section of the foreland was glaciated, it was likely by confluent Ayr Lake and Patricia Bay ice. The only evidence of glaciation is meltwater channels and erratic boulders. Numerous lateral meltwater channels exist in the region where the Kuvinilk River emerges from the foothills along the western edge of the foreland (Fig. 3). These channels define ice lobes that flowed out of the foothills and were likely derived from both Ayr Lake ice and Clyde Inlet ice that had converged in the valleys to the west. There are no moraines and no evidence for till cover of any kind, except for sporadic erratic boulders. Meltwater channels that dissect a ~200 m asl erratic-covered hill top ~10 km from the coast provide evidence for complete glaciation of the Kuvinilk River area at some time.

Northern Clyde Foreland

The low coastal landscape of the southern and central Clyde Foreland gives way to more hilly terrain between the Kogalu River and Eglinton Fiord (Fig. 3). Valleys were glaciated by Ayr Lake ice from the south and by Eglinton Fiord ice from the north. Shorelines demarcate ice-marginal lakes that formed in valleys draining northward into Eglinton Fiord (Fig. 3). At the timing of maximum ice cover, Eglinton and Ayr Lake ice were likely confluent and covered the whole region, as indicated by erratics covering the highest and most distal locations.

Marine shorelines

Two marine shorelines can be traced across the Clyde Foreland. The higher of the two, the marine limit at ~80 m asl, is degraded and discontinuous. The marine limit can be traced both north and south of the Clyde Foreland (e.g., Miller et al. 1977) and is most clearly traceable across the Aston Lowlands to the south (Fig. 1), where its most prominent expression is the Aston Delta (Løken 1966). The ~80 m marine limit is well dated to beyond the range of radiocarbon dating (Løken 1966; Miller et al. 1977; Mode 1980). On the Clyde Foreland, the ~80 m asl marine limit is best expressed in the Kuvinilk River area (Fig. 2). A lower elevation shoreline at ~22 m asl appears much fresher than the ~80 m asl marine limit, but because the 30–40-m-high Clyde Cliffs occupy most of the coastline, it can only be traced in a few areas across the Clyde Foreland. The ~22 m asl shoreline is best expressed as (1) a prominent beach in a protected cove

Table 1. Cosmogenic exposure ages from the glacially scoured zones on the Clyde Foreland (arranged from young to old per group).

Sample[a]	Site # on Fig. 5	Sample type	Sample height (m)	Latitude (N)	Longitude (W)	Elevation (m asl)	^{10}Be (10^5 atoms g^{-1})	^{26}Al (10^5 atoms g^{-1})	^{10}Be age (ka)	^{26}Al age (ka)	Weighted mean age and 1 S.D. uncertainty (ka)
Outer Clyde Inlet											
SIV1-00-3	1	Boulder	1.7	70°19.014′	68°51.416′	138	0.49±0.05	2.87±0.50	8.6±0.9	8.3±1.5	8.5±0.2
SIV1-00-4	1	Boulder	1.0	70°18.945′	68°51.702′	126	0.57±0.03	ND	10.2±0.5	ND	ND
SIV1-00-5	1	Boulder	3.0	70°18.933′	68°48.266′	42	0.59±0.02	ND	11.4±0.5	ND	ND
Patricia Bay lowland											
CF02-178	2	Cobble	0.0	70°26.339′	68°31.118′	231	0.71±0.05	ND	11.2±0.8	ND	ND
CF02-177	2	Cobble	0.0	70°26.630′	68°30.766′	252	0.70±0.04	ND	11.4±0.6	ND	ND
PB1-00-4	3	Boulder	1.5	70°27.841′	68°41.284′	145	0.59±0.09	4.85±0.66	10.3±1.3	14.0±1.7	11.7±2.6
PB1-00-3	3	Boulder	4.0	70°27.907′	68°40.899′	130	ND	4.41±0.48	ND	12.9±0.8	ND
PB3-00-4	4	Boulder	5.0	70°26.606′	68°45.343′	188	0.76±0.09	4.77±0.65	12.8±1.0	13.2±1.4	12.9±0.3
PB3-00-3	4	Boulder	1.5	70°26.993′	68°45.511′	192	1.07±0.11	6.65±0.82	18.0±1.1	18.3±1.6	18.1±0.2
Lower Kogalu River valley											
AL12-01-2	5	Boulder	1.2	70°42 19.1′	69°05 13.9′	36	0.55±0.03	ND	10.5±0.6	ND	ND
CF02-184	5	Cobble	0.0	70°42.431′	69°07.530′	40	0.61±0.06	ND	11.9±0.5	ND	ND
AL2-01-2	6	Boulder	1.5	70°35 05.6′	68°55 43.3′	220	0.87±0.03	ND	13.9±0.5	ND	ND
AL9-01-1	7	Boulder	3.0	70°41 29.4′	69°11 3.7′	178	0.88±0.03	ND	14.6±0.5	ND	ND
AL12-01-1	5	Boulder	10.0	70°42 23.2′	69°05 17.5′	52	0.81±0.03	ND	15.3±0.5	ND	ND
AL7-01-1	7	Boulder	5.0	70°41 7.4′	69°08 35.9′	93	0.86±0.05	ND	15.5±0.8	ND	ND
AL14-01-2	8	Boulder	0.8	70°37 35.9′	69°10 25.8′	45	0.89±0.04	ND	16.9±0.7	ND	ND
CF02-64	9	Boulder	5.0	70°36.823′	68°48.078′	98	0.94±0.09	ND	17.0±0.7	ND	ND
AL7-01-2	7	Boulder	2.5	70°40 58.3′	69°09 42.9′	130	0.99±0.03	ND	17.3±0.5	ND	ND
CF02-65	10	Boulder	3.0	70°38.812′	68°54.527′	85	1.22±0.11	ND	22.7±0.7	ND	ND
AL8-01-1	7	Boulder	1.0	70°41 29.9′	69°10 23.4′	172	1.39±0.07	ND	23.3±1.2	ND	ND
CF02-58	11	Cobble	0.0	70°34.843′	68°55.791′	300	1.58±0.05	ND	23.8±0.7	ND	ND
AL10-01-1	7	Boulder	3.8	70°41 31.1′	69°12 3.9′	185	1.45±0.13	ND	23.9±2.1	ND	ND
CF02-109	8	Cobble	0.0	70°37.482′	69°10.743′	50	2.59±0.22	ND	50.5±1.3	ND	ND
AL2-01-1	6	Boulder	1.5	70°35 16.4′	68°59 39.8′	208	4.54±0.16	ND	73.9±2.7	ND	ND
Upper Kogalu River valley											
AL4-01-2	12	Boulder	2.0	70°30 25.2′	68°55 42.6′	172	0.70±0.02	4.76±0.33	11.6±0.3	13.0±0.9	11.7±1.0
AL1-00–1	13	Cobble	0.0	70°29.336′	69°21.235′	259	0.79±0.03	4.69±0.25	12.6±0.3	11.7±0.6	12.4±0.6
CF02-107	14	Cobble on Boulder	1.5	70°37.129′	69°14.06′	124	0.72±0.07	ND	12.9±0.5	ND	ND
AL4-01-1	12	Boulder	2.5	70°30 43.6′	68°55 29.3′	153	0.82±0.02	4.53±0.25	14.0±0.4	12.7±0.7	13.7±0.9
AL6-01-2	15	Boulder	1.5	70°30 38.3′	69°02 18.1′	190	0.85±0.03	ND	13.9±0.4	ND	ND
AL6-01-1	15	Boulder	2.5	70°30 40.4′	69°02 17.4′	207	1.63±0.04	ND	26.2±0.6	ND	ND
Eglinton Fiord											
CF02-91	16	Boulder	2.0	70°42.812′	69°20.861′	134	0.78±0.07	ND	13.7±0.6	ND	ND

Table 1 (*concluded*).

Sample[a]	Site # on Fig. 5	Sample type	Sample height (m)	Latitude (N)	Longitude (W)	Elevation (m asl)	^{10}Be (10^5 atoms g^{-1})	^{26}Al (10^5 atoms g^{-1})	^{10}Be age (ka)	^{26}Al age (ka)	Weighted mean age and 1 S.D. uncertainty (ka)
Laboratory replicates											
BDF-00-2[b]	NA	Bedrock	0.0	70°16.500′	68°58.403′	36	0.49±0.04	ND	9.4±0.4	ND	ND
BDF-00-2[b]	NA	Bedrock	0.0	70°16.500′	68°58.403′	36	0.49±0.04	ND	9.3±0.4	ND	ND
TM1-00-1[b]	NA	Bedrock	0.0	70°17.913′	69°08.822′	605	1.99±0.17	ND	22.1±0.5	ND	ND
TM1-00-1[b]	NA	Bedrock	0.0	70°17.913′	69°08.822′	605	1.99±0.17	ND	21.9±1.4	ND	ND
CF02-68	51	Cobble	0.0	70°43.769′	69°09.191′	120	3.97±0.13	ND	70.8±2.3	ND	ND
CF02-68	51	Cobble	0.0	70°43.769′	69°09.191′	120	4.36±0.11	ND	77.8±1.9	ND	ND

Note: ND = no data; S.D., standard deviation.
[a]For samples with a complex exposure and burial history, these are only apparent ages calculated from the total exposure history preserved in a sample.
[b]Samples are from the Clyde Region but outside of the study area reported here.

in northernmost Clyde Foreland, (2) a ~22 m asl delta that is fed by a prominent meltwater channel, also along the northern foreland coast, and (3) well-preserved outwash terraces along the Kuvinilk River that grade to ~23 m asl at the modern coastline (Fig. 3).

Reconstruction of basal ice thermal regimes

Erratics and meltwater channels occur across the entire foreland, documenting complete glaciation of the foreland at some time. However, different sectors of the foreland contain different types of glacial features. For example, moraines are restricted to the most ice-proximal locations (around Patricia Bay and the mouth of Ayr Lake), and only erratics and sparse meltwater channels occupy the most ice-distal locations. More ice-sheet modification of the landscape has occurred where ice was topographically confined (flowing through Patricia Bay from Clyde Inlet and through the Ayr Lake trough; Fig. 4), likely indicating the presence of warm-based erosive ice. Where the ice lobes became unconfined and spread outward across the foreland, progressively less erosion took place, and ice margins likely became cold-based, as indicated by lateral meltwater channels (e.g., Dyke 1999; Fig. 4). The two major pathways of ice across the foreland, along the Kogalu River valley and in the Patricia Bay lowland, have a higher lake density than other sectors of the foreland (Fig. 2), consistent with the inference that these valleys held the thickest ice and experienced either more glacial scour (cf. Sugden 1978; Andrews et al. 1985) or have more hummocky ground moraine.

The differential preservation of the two shorelines on the Clyde Foreland provides further insight into basal ice thermal regimes. Unlike the ~80 m asl marine limit, which is degraded and in most places littered with erratics, features that compose the ~22 m asl shoreline distinctly lack a cover of erratics. The ~80 m asl marine limit is preserved in those locations that lack any indication of erosive ice (e.g., the Kuvinilk River valley; Fig. 3), suggesting that the ~80 m asl marine limit existed prior to the most recent glaciation of the Clyde Foreland and was preserved where ice was frozen to its bed and removed where ice was more erosive.

The Clyde Foreland can be subdivided into two main landscape types (Fig. 5): glacially scoured landscapes (moraines and signs of scouring) and unscoured landscapes that do not appear to have been modified by ice (presence of meltwater channels and erratics, but lack of evidence of scouring). We interpret the spatial distribution of glacially scoured versus unscoured landscapes as representing former basal ice thermal regimes. The ice sheet was erosive, more dynamically active, and perhaps warm-based in the scoured regions and was non-erosive, less dynamically active, and likely frozen-bedded in the unscoured areas (Fig. 5).

Results and interpretations of cosmogenic exposure ages

Erratics from glacially scoured landscapes (Patricia Bay lowland, Kogalu River valley, and areas proximal to Eglinton Fiord) yield almost exclusively LGM (we consider CE ages of 15 ± 2 ka to represent deglaciation from the LGM ice advance) or younger CE ages (Fig. 6; Tables 1, 2). In contrast, erratics from unscoured landscapes (distal regions

Fig. 4. Aerial photographs of the Clyde Foreland (locations shown in Fig. 3). (A) Section of glacially scoured terrain showing high lake density from glacial scour and (or) hummocky ground moraine. The ice lobes diverged around the high massif in the center of the photograph. A well-defined ice margin can be seen in the bottom right corner of the photograph. (B) Section of glacially unmodified terrain showing dozens of lateral meltwater channels that depict a cold-based ice lobe retreating from the upper Clyde River drainage area. An ice lobe spilled into this valley from Clyde Inlet by overflowing a low drainage divide. The aerial photographs A-16213-52 (A) and A-16213-56 (B) © 1958. Her Majesty the Queen in Right of Canada, reproduced from the collection of the National Air Photo Library with permission of Natural Resources Canada.

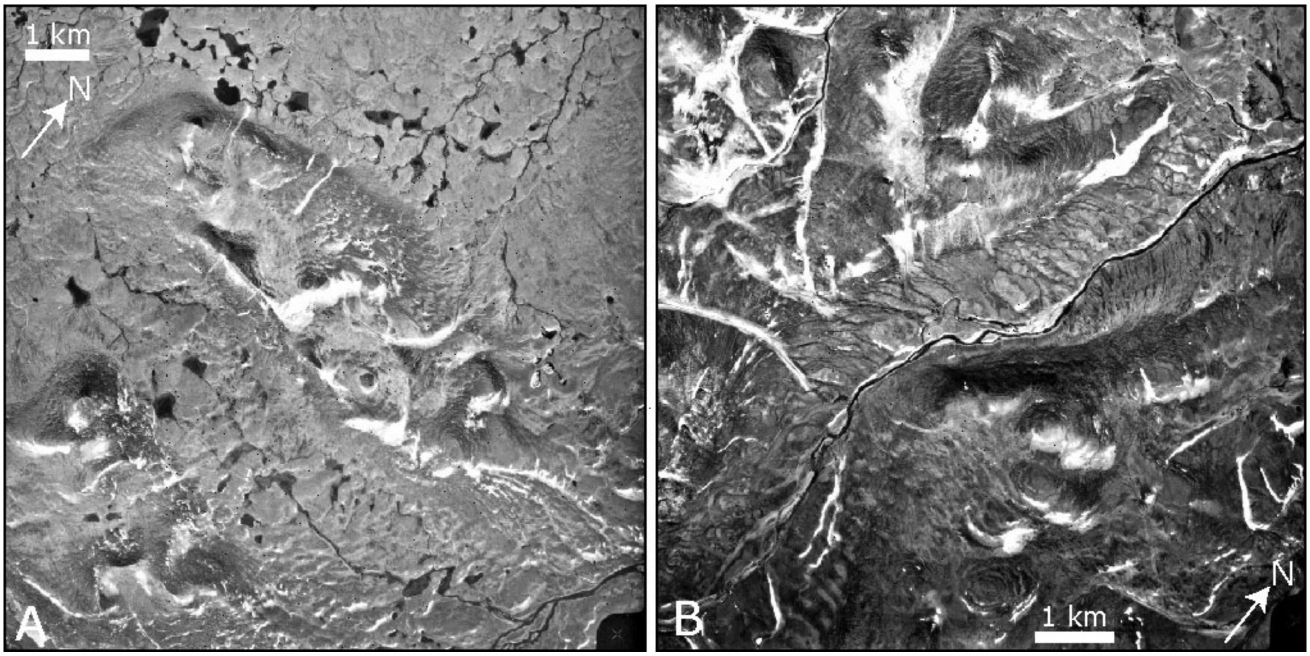

Fig. 5. Map of Clyde Foreland showing conceptual picture of the diminishing efficiency of glacial erosion as the LIS spills onto the foreland. Zones with shading are categorized as the "scoured zone," and the parts of the foreland left white are categorized as the "unscoured zone." Numbers refer to locations of CE ages (Tables 1, 2).

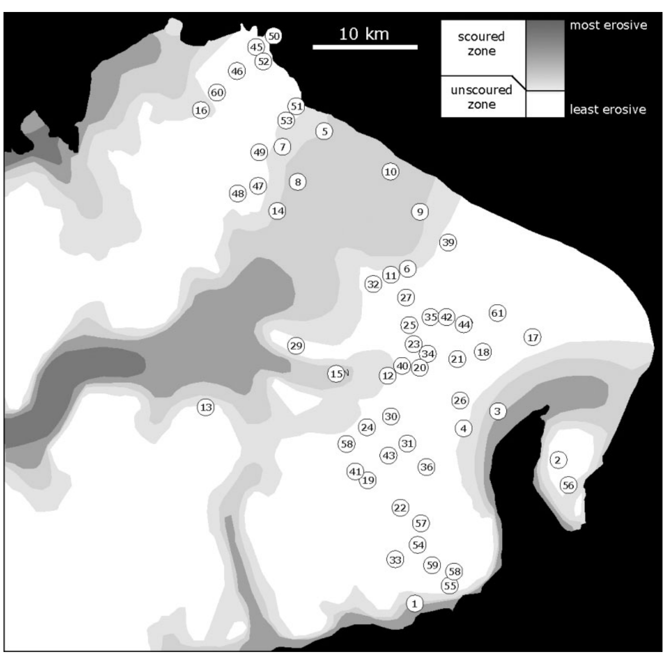

and high-elevation areas) display a wide range of older CE ages along with LGM and deglacial CE ages. For example, whereas 77% of the ages from the scoured areas are < 17 ka, only 32% of the ages from the unscoured areas are < 17 ka (Fig. 6). The single-mode distribution of the ages from scoured landscapes leads to a straight-forward interpretation relative to the multimodal distribution of ages from unscoured areas.

Glacially scoured landscapes

Three broad regions of our field area contain signs of dynamically active ice: lowlands proximal to Patricia Bay, lowlands along the Kogalu River proximal to Ayr Lake, and lowlands proximal to Eglinton Fiord (Fig. 5). Three boulders from the moraines around Patricia Bay average 12.5 ± 0.7 ka (Fig. 7), excluding one ~18 ka outlier. Two erratics at an elevation of 250 m asl on the northern flank of Black Bluff have CE ages of ~11.2 ka. Farther up the fiord, a tributary valley of outer Clyde Inlet contains a lateral moraine that dates to 10.0 ± 1.5 ka (n = 3). Cosmogenic exposure ages from erratics in the lower Kogalu River valley have two different modes (Figs. 6, 7): eight erratics average 15.3 ± 1.8 ka, and four erratics average 23.5 ± 0.1 ka. Two erratics predate the LGM at 73.9 ± 2.7 and 50.5 ± 1.3 ka, and one boulder yielded an anomalously young CE age of 10.5 ± 0.6 ka. Five CE ages from lateral ice margins farther up valley average 13.0 ± 1.0 ka, excluding an old outlier of 26.2 ± 0.6 ka. One erratic from the scoured lowland adjacent to Eglinton Fiord has an age of 13.7 ± 0.6 ka.

We interpret CE ages from the three glacially scoured regions of the Clyde Foreland (Fig. 6A) as evidence that deglaciation took place between ~12 and 15 ka (Figs. 5, 6; Table 1). The 10 ka moraine in outer Clyde Inlet suggests that, following ice recession from the foreland, ice retreated from outer Clyde Inlet ~10 ka. The bimodal distribution of exposure ages from coastal Kogalu River valley is difficult to explain. It is likely that ice flowing along the Kogalu River valley became less erosive as it flowed from the Ayr Lake trough to the outer coast. Thus, perhaps the advance that deposited the ~15 ka erratics overran but did not disturb the ~24 ka erratics. Marsella et al. (2000) obtained a similar bimodal age distribution from the type Duval moraine on southern Baffin Island, and raised the possibility that the moraine represented two advances during the LGM. The older samples (>25 ka; n = 3) in the Kogalu River valley are interpreted to have inheritance from a period or periods of exposure prior to the LGM.

The abundance of erratics with CE ages between 12 and 15 ka indicates that the LIS crossed the scoured areas Clyde Foreland during the LGM. However, the efficiency of glacial erosion decreased as ice flowed farther along the foreland (Fig. 5). Glaciomarine deposits that cap the Clyde Cliffs bordering the Kogalu River valley are beyond the range of radiocarbon dating (Miller et al. 1977). These results indicate that the LIS crossed the Clyde Cliffs in the Kogalu River valley during the LGM, but did not deposit a till and left the surface sediments largely undisturbed.

Unscoured landscapes

Seventy-two CE ages were obtained on erratics from unscoured landscapes in the Clyde region (Figs. 5, 6B). Samples include large (>2 m × 2 m × 2 m) erratic boulders (n = 38; Fig. 8), cobbles from terraces, kames, and marine deposits, or perched on erratic boulders (n = 23), and one sample of pebbles from a marine deposit. The youngest mode of CE ages (14.7 ± 2.7 ka, n = 26; Fig. 6B) from the unscoured areas overlaps with the youngest mode of CE ages from the scoured areas (12.7 ± 1.5 ka, n = 19; Fig. 6A). The largest concentration of samples from unscoured areas is from the Kuvinilk River valley (Figs. 5, 6), where the CE ages are strikingly different from erratics within the scoured zones. Thirteen of 46 erratics (28%) have ages < 17 ka, in contrast to a higher percentage (77%) of ages < 17 ka in the scoured terrain on either side (Fig. 6A). Most of the pre-LGM erratics fall into clusters: 38–46 (n = 9; 20%), 30–35 (n = 8; 17%), and 20–25 ka (n = 5; 11%). Eight erratics (17%) are > 46 ka. There are no relationships between age and sample type, sample height, or sample location (e.g., elevation, distance along flowline; Tables 1, 2; Fig. 5). Two of 11 erratics from the Eglinton unscoured region are ~12 ka, two samples fall in the 38–46 ka cluster from the Kuvinilk River valley, and four are older. Because of the complexity in the CE age distribution from the unscoured lowlands, we present our interpretations as follows.

Eleven erratics from the upland summits ≥450 m asl on either side of Patricia Bay include one CE age in the 38–46 ka cluster and the remainder compose two modes at 18.5 ± 1.0 ka (n = 5) and 12.0 ± 1.9 (n = 5). Cosmogenic exposure ages of the upland bedrock upon which erratics are perched range from ~60 to 80 ka, indicating that the erratics were deposited by non-erosive ice (Briner et al. 2003). These erratcis provide important constraints on ice thickness. The younger CE age cluster at ~12 ka from the summit erratics (n = 5), which overlaps with the deglaciation age of Patricia Bay (~12 ka), and is slightly older than the moraine in outer Clyde Inlet (~10 ka), indicates the timing of upland deglaciation. Thus, these summits were covered by cold-based Laurentide ice that reached ≥450 m asl until deglaciation at ~12 ka (Briner et al. 2003). The older age cluster at ~18.5 ka (n = 5) is more difficult to interpret, but perhaps the erratics were deposited during some prior period of upland deglaciation, and were overrun by a non-erosive ice advance that deposited the 12-ka erratics.

Marine features

Four samples were collected from the ~80 m asl marine limit. Two cobbles from south of outer Eglinton Fiord have CE ages of 40.7 ± 1.0 and 29.5 ± 0.8 ka. A third cobble from north of the Kogalu River mouth has a CE age of 40.9 ± 1.0 ka, and a collection of pebbles from a marine feature near the Kuvinilk River have an integrated CE age of 42.6 ± 1.2 ka. Excluding the 29.5 ka outlier, these samples have an average age of 41.1 ± 1.0 ka (n = 3), which overlaps with the cluster of erratic CE ages at 38–46 ka (Fig. 6).

Discussion

Cosmogenic exposure dating complexities

The CE ages of erratics in the glacially scoured terrain are dominantly from LGM deglaciation (~12–17 ka), with a secondary mode ~24 ka and a few outliers apparently with inheritance. However, the pattern of CE ages from the unscoured regions exhibits far more variability (Fig. 6). Three main lines of evidence demonstrate that the observed age scatter is not an artifact of analytical uncertainty, but reflects actual differences in exposure history. First, analytical uncertainty of individual (average 4%) and replicate analyses (average 3%) is far below that required to explain the CE age scatter (Table 1). Second, procedural blanks are consistent between sample batches (see "Cosmogenic exposure dating methods"), suggesting that the observed variability is not a laboratory methodological problem. Finally, the wide distribution of CE ages mainly occurs in terrains that lack evidence of erosive ice, in stark contrast to adjacent glacially scoured landscapes.

The exposure history (total cosmogenic nuclide concentration) of erratics on the Clyde Foreland can be influenced by several factors that can lead to CE ages that both predate and postdate the timing of erratic deposition. Isotopic inheritance can occur when an ice sheet deposits erratics that have a prior cosmogenic nuclide inventory and will yield a CE age that is *older* than when an erratic was deposited. Inheritance may arise by recycling boulders that have a prior exposure history or transporting supraglacial rockfall debris that is deposited with a previously exposed face in the skyward direction. Inheritance is assumed to lead to a random distribution of anomalously old CE ages.

Other factors can lead to CE ages *younger* than the timing of deposition. Some erratics on the Clyde Foreland may have been emplaced prior to the LGM and have since experienced prolonged periods of shielding by permanent snow cover, by cold-based local ice, or by cold-based Laurentide

Fig. 6. (A) Relative probability plots of CE ages from erratics from the three glacially scoured regions and of the unscoured sample sets. Asterisks show which sample sets have ages >80 ka that fall outside of the histogram. (B) Relative probability plots of CE ages separated into glacially scoured areas and unscoured areas. Note that the bottom axis is labeled “age,” but cosmogenic nuclide concentrations from samples that have complex exposure histories yield only *apparent* ages. Vertical shaded bars represent the timing of deglaciation (10–17 ka) and the hypothesized timing of a major penultimate advance (38–46 ka; see text).

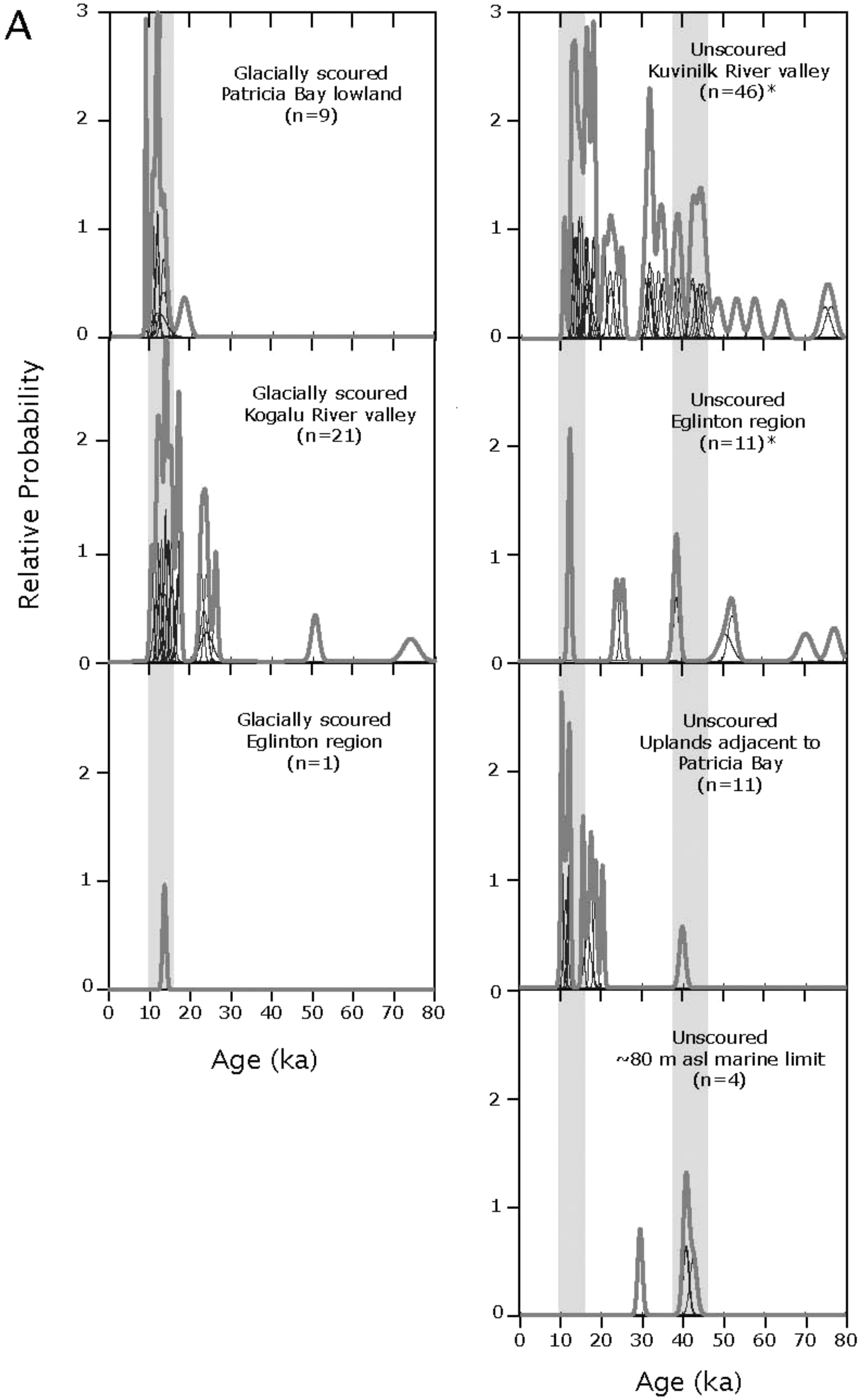

Fig. 6 (*concluded*).

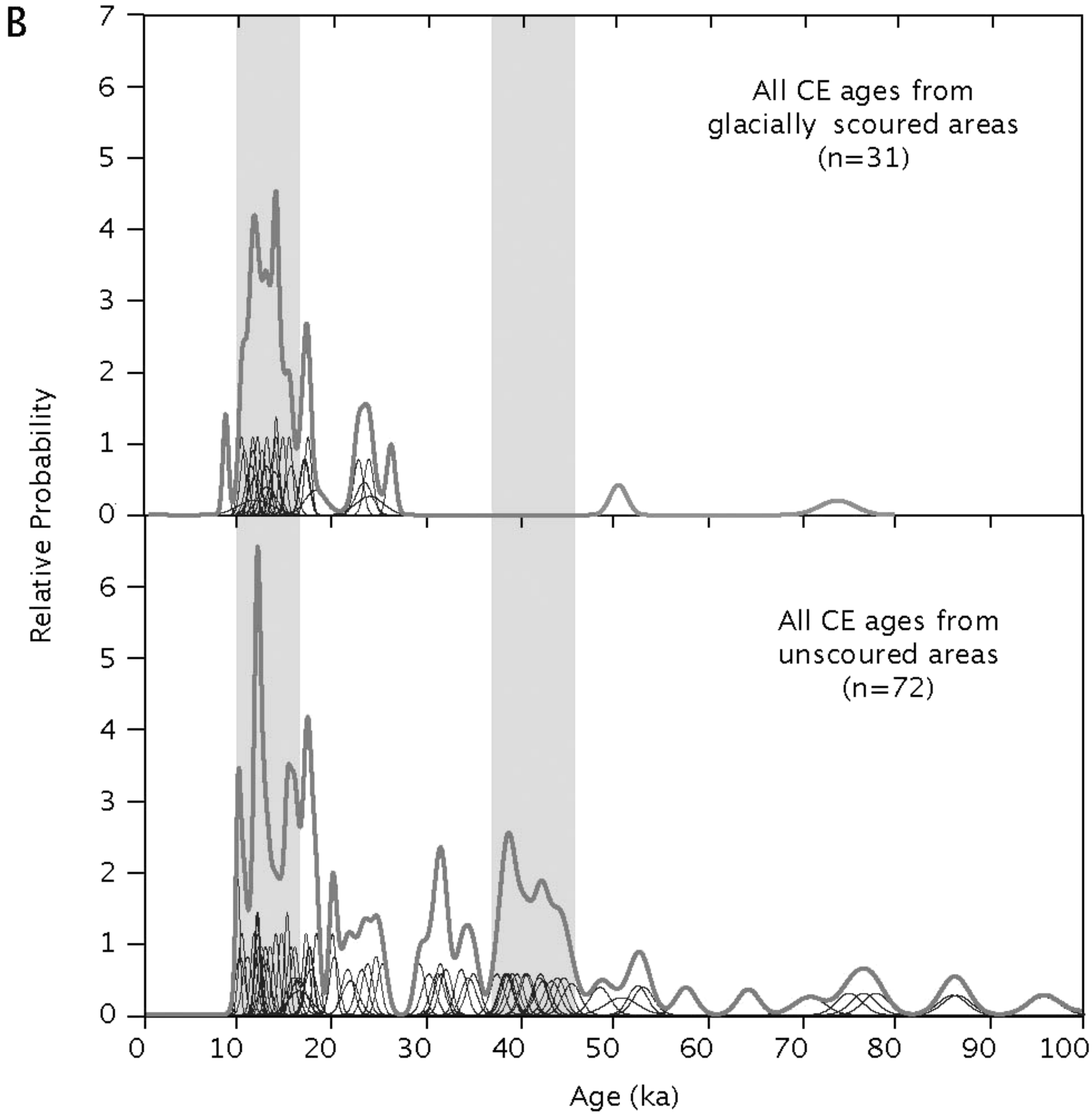

ice. While we do not consider shielding an important factor in the Holocene, it is possibly significant prior to the Holocene. Shielding would either partially or completely attenuate cosmogenic nuclide production and result in apparent CE ages younger than the timing of their original deposition.

In a landscape that was covered by both erosive and non-erosive ice, erratics may have a complex exposure and burial history. It has been documented that delicate tors can survive beneath cold-based ice (e.g., André 2004; Bierman et al. 2001; Briner et al. 2003; Hall and Glasser 2003; Marquette et al. 2004). Thus, it is possible that large erratic boulders can survive cold-based ice cover as well. In this case, CE ages underestimate the timing of erratic emplacement because erratics are shielded by one or more episodes of cold-based ice cover. Therefore, a wide range in CE ages might be expected in a landscape covered, but not modified, by cold-based ice.

Glacial history of the unscoured areas

The probability plots of CE ages (Fig. 6) provide information on the glacial history of the unscoured areas. Most of the CE ages in unscoured landscapes fall into discrete clusters (38–46, 30–35, 20–25, and 12–17 ka), with a small number of outliers. Three possible interpretations are (1) all erratics were deposited during the LGM, and the wide distribution arises from differential inheritance, (2) all erratics were deposited during a single advance prior to the LGM, and the wide distribution arises from differential post-depositional modification, or (3) the erratics were deposited during multiple cold-based ice advances. We rule out the

Table 2. Cosmogenic exposure ages from the glacially unmodified zones on the Clyde Foreland (arranged from young to old per group).

Sample[a]		Sample type	Sample height (m)	Latitude (N)	Longitude (W)	Elevation (m asl)	^{10}Be (10^5 atoms g^{-1})	^{26}Al (10^5 atoms g^{-1})	^{10}Be age (ka)	^{26}Al age (ka)	Weighted mean age and 1 S.D. uncertainty (ka)
Kuvinilk River basin											
CF02-4	17	Cobble	0.0	70°31.613′	68°35.938′	82	0.55±0.03	ND	10.7±0.5	ND	ND
CF02-59	18	Boulder	4.0	70°35.127′	68°50.490′	142	0.72±0.03	ND	12.4±0.4	ND	ND
CF02-146	19	Cobble	0.0	70°25.339′	68°59.300′	368	0.93±0.05	ND	12.8±0.6	ND	ND
CF3-01-1	20	Boulder	4.0	70°33′ 33.6″	68°51′ 38.8″	135	0.77±0.02	4.56±0.22	13.3±0.4	13.0±0.8	13.2±0.2
PB6-01-2	21	Boulder	2.0	70°31′ 48.5″	68°44′ 53.4″	136	0.76±0.05	ND	13.2±0.8	ND	ND
CF02-125	22	Cobble	0.0	70°23.280′	68°56.031′	293	0.93±0.04	ND	13.7±0.6	ND	ND
CF02-20	18	Boulder	4.0	70°33.876′	68°53.462′	155	0.84±0.03	ND	14.3±0.5	ND	ND
CF02-23	23	Boulder	0.4	70°31.351′	68°50.291′	140	0.87±0.03	ND	14.9±0.5	ND	ND
CF02-6	17	Boulder	0.6	70°31.858′	68°35.469′	82	0.87±0.03	ND	15.9±0.6	ND	ND
CF02-164	24	Boulder on boulder	3.4	70°27.752′	68°59.788′	444	1.27±0.08	ND	16.2±1.1	ND	ND
CF02-21	25	Boulder	2.5	70°32.658′	68°51.240′	149	0.96±0.03	ND	16.3±0.6	ND	ND
PB4-00-1	26	Boulder	8.0	70°28.168′	68°45.876′	215	1.09±0.11	7.34±1.14	17.9±1.1	19.8±2.5	16.7±1.1
PB5–01–1	27	Boulder	1.0	70°30 35.4′	68°42 59.8′	149	0.99±0.10	ND	16.8±1.7	ND	ND
CF02-12	28	Boulder	0.4	70°32.925′	68°47.659′	211	1.11±0.04	ND	17.8±0.6	ND	ND
CF02-5	17	Cobble	0.0	70°31.815′	68°35.658′	82	0.98±0.03	ND	17.9±0.6	ND	ND
PB5-01-2	27	Boulder	1.3	70°30 49.5′	68°43 10.2′	143	1.06±0.05	ND	18.0±0.9	ND	ND
CF02-47	29	Boulder	3.0	70°31.305′	69°05.061′	406	1.53±0.13	ND	20.5±0.7	ND	ND
CF02-152	30	Cobble on boulder	5.0	70°27.854′	68°56.001′	269	1.44±0.06	ND	21.9±0.9	ND	ND
CF02-154	30	Boulder	1.5	70°28.325′	68°55.142′	344	1.58±0.09	ND	22.2±1.2	ND	ND
CF02-26	23	Boulder	4.0	70°31.067′	68°49.354′	122	1.33±0.05	ND	23.4±0.9	ND	ND
CF02-157	31	Boulder	0.5	70°27.504′	68°54.093′	240	1.60±0.04	ND	24.9±0.7	ND	ND
CF02-51	32	Boulder	3.0	70°32.374′	69°55.683′	190	1.86±0.06	ND	30.5±1.0	ND	ND
SIV6-00-1	33	Boulder	4.0	70°21.340′	68°55.222′	267	2.03±0.05	ND	31.4±1.0	ND	ND
CF2-01-2	34	Boulder	2.5	70°31′ 51.6″	68°51′ 06.6″	137	1.83±0.05	ND	31.7±0.8	ND	ND
SIV6-00-2	33	Boulder	1.5	70°21.391′	68°55.339′	270	2.04±0.05	ND	31.8±1.0	ND	ND
CF02-14	28	Boulder	1.5	70°32.926′	68°48.186′	218	2.02±0.05	ND	32.3±0.9	ND	ND
CF02-13	28	Boulder	1.3	70°32.989′	68°48.155′	224	2.13±0.06	ND	33.9±0.9	ND	ND
CF02-7	35	Cobble	0.0	70°33.173′	68°36.378′	95	1.91±0.06	ND	34.7±1.1	ND	ND
CF2-01-1	34	Boulder	3.4	70°30′ 39.1″	68°48′ 16.1″	132	2.02±0.06	ND	35.2±1.0	ND	ND
CF02-22	36	Boulder	1.0	70°32.096′	68°42.299′	151	2.20±0.06	ND	37.7±1.0	ND	ND
CF02-130	37	Boulder	0.5	70°25.555′	68°51.261′	240	2.47±0.06	ND	38.6±1.0	ND	ND
CF02-163	38	Boulder	3.0	70°26.632′	69°00.677′	376	2.87±0.07	ND	39.3±1.0	ND	ND
CF02-63	39	Boulder	1.5	70°36.042′	68°45.862′	245	2.71±0.07	ND	42.2±1.1	ND	ND
CF02-147	19	Cobble	0.0	70°25.339′	68°59.300′	368	3.00±0.07	ND	42.3±1.0	ND	ND
CF02-15	28	Cobble on CF02-16	1.5	70°33.005′	68°48.466′	218	2.72±0.07	ND	43.5±1.2	ND	ND
CF02-18	18	Boulder	6.0	70°34.216′	68°52.914′	145	2.55±0.07	ND	44.1±1.1	ND	ND
AL3-01-1	40	Cobble	0.0	70°30 56.8′	68°51 54.4′	132	2.56±0.06	ND	44.8±1.1	ND	ND
CF02-162	41	Boulder	1.0	70°25.720′	68°00.068′	400	3.40±0.10	ND	45.6±1.3	ND	ND
CF1-01-1	42	Pebbles on boulder	1.5	70°33′ 27.3″	68°46′ 22.3″	107	2.71±0.08	ND	48.6±1.5	ND	ND
CF02-153	30	Cobble on boulder	4.0	70°28.152′	68°56.036′	366	3.83±0.11	ND	53.2±1.5	ND	ND
CF02-161	43	Cobble	0.0	70°26.369′	68°57.013′	292	4.38±0.11	ND	57.7±1.5	ND	ND

Table 2 (*concluded*).

Sample[a]		Sample type	Sample height (m)	Latitude (N)	Longitude (W)	Elevation (m asl)	^{10}Be (10^5 atoms g^{-1})	^{26}Al (10^5 atoms g^{-1})	^{10}Be age (ka)	^{26}Al age (ka)	Weighted mean age and 1 S.D. uncertainty (ka)
CF02-16	28	Boulder	1.5	70°33.005′	68°48.466′	218	4.00±0.10	ND	64.3±1.6	ND	ND
CF02-54	32	Boulder	2.5	70°34.702′	69°56.769′	361	5.24±0.44	ND	75.0±1.9	ND	ND
CF02-27	23	Boulder	1.5	70°31.042′	68°49.283′	121	4.29±0.11	ND	76.5±1.9	ND	ND
CF02-10	44	Boulder	2.5	70°32.880′	68°38.903′	143	4.92±0.12	ND	85.9±2.1	ND	ND
PB6-01-1	21	Boulder	1.0	70°31′57.7″	68°45′57.5″	117	7.07±0.17	37.3±1.3	128.0±3.0	113.7±6.1	125.2±10.1
Eglinton region											
CF02-86	45	Boulder	3.0	70°46.307′	69°14.350′	46	0.64±0.06	ND	12.4±0.5	ND	ND
CF02-87	46	Boulder	1.5	70°45.359′	69°18.737′	67	0.67±0.06	ND	12.5±0.6	ND	ND
CF02-38	47	Cobble on boulder	6.0	70°41.027′	69°15.081′	211	1.49±0.13	ND	24.0±0.8	ND	ND
CF02-35	48	Boulder	1.0	70°41.022′	69°20.285′	155	1.49±0.13	ND	25.6±0.8	ND	ND
CF02-92	49	Boulder	2.5	70°42.006′	69°15.571′	263	2.53±0.7	ND	38.7±1.0	ND	ND
CF02-82	50	Cobble	0.0	70°46.784′	69°12.966′	150	2.27±0.06	ND	38.9±1.0	ND	ND
CF02-67	51	Cobble	0.0	70°43.769′	69°09.191′	120	2.87±0.14	ND	50.9±2.4	ND	ND
CF02-77	52	Cobble	0.0	70°45.173′	69°13.135′	61	2.76±0.23	ND	52.6±1.4	ND	ND
CF02-68	51	Cobble	0.0	70°43.769′	69°09.191′	120	3.97±0.13	ND	70.8±2.3	ND	ND
CF02-68d	51	Cobble	0.0	70°43.769′	69°09.191′	120	4.36±0.11	ND	77.8±1.9	ND	ND
CF02-83	50	Cobble-granite	0.0	70°46.784′	69°12.966′	150	4.98±0.12	ND	86.4±2.1	ND	ND
AL11-01-1	53	Cobble	0.0	70°42 32.9′	69°08 39.9′	118	5.32±0.13	ND	95.6±2.3	ND	ND
Uplands adjacent to Patricia Bay											
CF02-118	54	Cobble	0.0	70°22.292′	68°50.760′	543	0.88±0.03	ND	10.3±0.3	ND	ND
SIV7-01-3	55	Boulder	0.5	70°20.000′	68°48.042′	464	0.81±0.02	5.33±0.30	10.1±0.3	11.0±0.4	10.5±0.7
SIV7-00-2	55	Cobble	0.0	70°19.993′	68°48.015′	462	0.85±0.04	6.34±0.24	10.8±1.1	13.2±2.1	11.3±1.7
CF02-30	56	Boulder	1.0	70°25.421′	68°28.349′	430	0.93±0.04	ND	12.0±0.5	ND	ND
CF02-120	57	Cobble	0.0	71°23.157′	69°50.980′	610	1.13±0.03	ND	12.3±0.4	ND	ND
SIV9-01-2	58	Boulder	0.5	70°20.366′	68°46.418′	520	1.30±0.03	ND	15.5±0.4	ND	ND
SIV8-01-2	58	Boulder	0.5	70°20.115′	68°46.747′	504	1.46±0.05	7.97±0.44	17.5±0.6	15.8±0.6	16.7±1.2
CF02-31	56	Cobble	1.0	70°25.537′	68°29.675′	380	1.29±0.03	ND	17.5±0.5	ND	ND
CF02-119	57	Boulder	0.5	70°23.157′	68°50.980′	610	1.69±0.05	ND	18.6±0.5	ND	ND
CF02-117	54	Boulder	0.5	70°22.292′	68°50.760′	543	1.74±0.04	ND	20.3±0.5	ND	ND
CF02-115	59	Cobble	0.0	70°21.212′	68°48.671′	426	3.04±0.08	ND	39.8±1.0	ND	ND
~80-m asl marine limit											
CF02-89	60	Cobble	0.0	70°44.491′	69°20.824′	82	1.57±0.13	ND	29.5±0.8	ND	ND
CF02-40	51	Cobble	0.0	70°42.786′	69°08.785′	85	2.22±0.02	ND	40.9±1.0	ND	ND
CF02-88	60	Cobble	0.0	70°44.491′	69°20.824′	82	2.16±0.02	ND	40.7±1.0	ND	ND
CF02-8	61	Pebbles	0.0	70°11.173′	68°36.378′	90	2.35±0.07	ND	42.6±1.2	ND	ND

Note: ND, no data; S.D., standard deviation.
[a]For samples with a complex exposure and burial history, these are only apparent ages calculated from the total exposure history preserved in a sample.

Fig. 7. Photographs of sampled boulders from glacially scoured terrain. (A) Sample AL7-01-1 from the north side of the outer Kogalu River valley at 93 m asl (site 5, Fig. 5) has an exposure age of 15.5 ± 0.8 ka. (B) Sample PB1-00-4 from the innermost moraine adjacent to Patricia Bay has an average age of 11.7 ± 2.6 ka (site 2, Fig. 5).

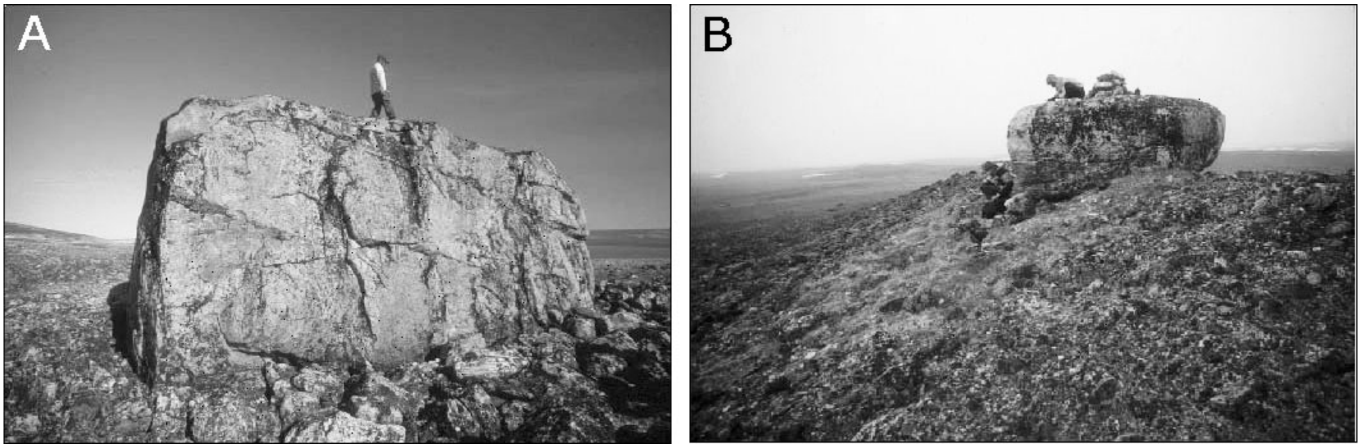

Fig. 8. Photographs of erratic boulders from glacially unmodified terrain of the Kuvinilk River basin. (A) CF3-01-1 at 135 m asl has an exposure age of 13.2 ± 0.2 ka (site 24, Fig. 5). (B) CF2-01-2 at 137 m asl has an exposure age of 31.7 ± 0.8 ka (site 23, Fig. 5).

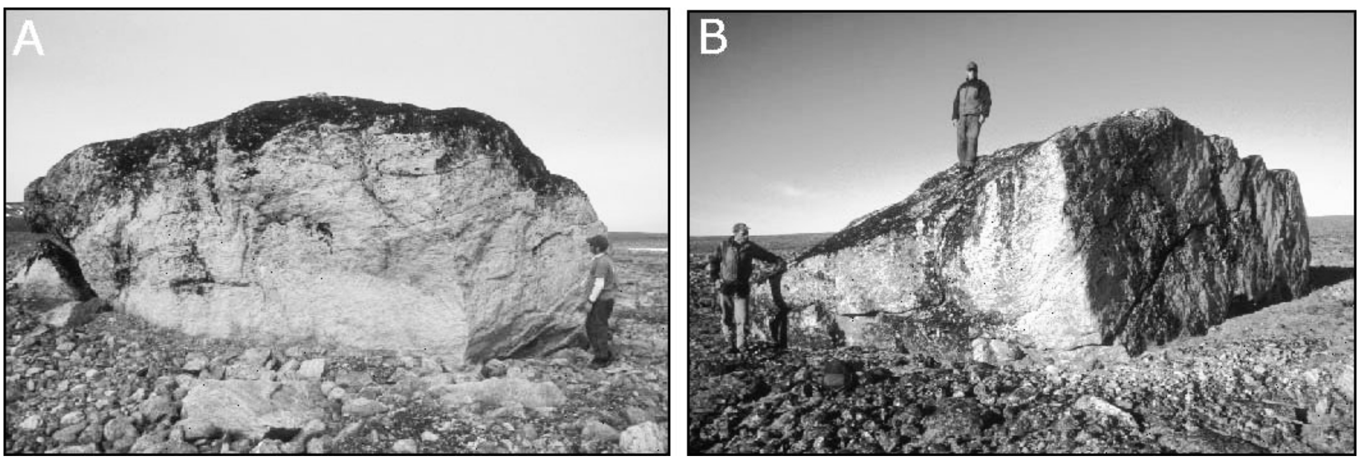

first interpretation because the clustering in CE ages is unlikely to arise from inheritance. We rule out the second interpretation because none of the CE ages on the foreland are younger than ~11 ka, indicating that post-depositional rolling is unlikely. Thus, we favor the third interpretation that the erratics were deposited on the Clyde Foreland during several different cold-based glacial advances, where each advance deposited a new suite of erratics without disturbing many of the previously deposited erratics. Hence, the CE age clusters may represent specific intervals of erratic deposition.

The CE ages of the 80-m asl marine limit cluster at ~41 ka. These ages are minimum estimates because of an unknown period of burial, either by cold-based Laurentide ice or by a local snowpack. Miller et al. (1977) assigned the ~80-m asl shoreline to MIS 5a (~80 ka) based on diagnostic thermophilous mollusks that occur in regressional shorelines. Greenland ice core paleotemperature reconstructions support this interpretation as the most recent time when marine conditions might have been relatively warm (Dansgaard et al. 1993). If this age is correct, then the ~80-m asl shoreline has been shielded for a total duration of ~40 thousand years, and exposed for ~25 thousand years prior to the last deglaciation. The erratic CE age cluster at ~38–46 ka, which overlaps with the ~80 m asl marine limit CE ages, likely records deglaciation from a major ice advance that transported erratics onto the Clyde Foreland. Isostatic depression from this advance explains the 80 m asl marine limit. The CE age clusters at 30–35, 20–25, and 12–17 ka indicate at least three subsequent cold-based ice advances to the foreland since MIS 5a. This scenario requires that unscoured landscapes on the Clyde Foreland have been overrun numerous times by a cold-based LIS since ~80 ka.

A remaining question concerns the history of the unscoured regions during the LGM. Thirteen of the 46 samples (28%) fall in the ~12–17 ka age cluster that represents the deglaciation of the adjacent scoured lowlands. In contrast, >50% of the CE erratic ages from the upland unscoured zones closer to Clyde Inlet are ≤15 ka, and 81% are < 19 ka. The relatively low percentage of deglacial-age erratics in the unscoured lowlands possibly indicates that the most distal lowlands remained ice free during the LGM. In this case, explaining the 12 deglacial-age erratics is difficult; perhaps these young ages are the result of shielding by permanent snowfields and local cold-based ice carapaces or were delivered during the LGM via mass wasting (e.g., slushflow) at the ice front. We cannot conclusively support the presence or absence of the LIS on the unscoured lowlands during the LGM, but suggest that cold-based LIS lobes covered the unscoured areas several times since ~80 ka.

Implications

Ice-sheet history

Our finding of a more extensive LIS on the Clyde Foreland during the LGM than previously depicted (e.g., Løken 1966; Miller et al. 1977; Dyke and Prest 1987; Dyke et al. 2002) agrees with other recent reconstructions of relatively more extensive ice in the Clyde region. Meltwater channels dominate the Aston Lowlands (Fig. 1), to the south of the Clyde Foreland, implying that it was also largely covered by cold-based ice (Coulthard 2003). Only in those areas most proximal to where ice spilled onto the lowlands from adjacent fiords does it appear to have been scoured by the LIS (Coulthard 2003). Recent cosmogenic exposure ages from erratics on the surface of the 80-m asl, >54 ka Aston Delta indicate that non-erosive ice completely covered the delta, and by inference most of the Aston Lowlands, during the LGM (Davis et al. 2002).

Cosmogenic exposure dating campaigns on southern Baffin Island have also shown complexities in cosmogenic nuclide data sets (e.g., Marsella et al. 2000; Bierman et al. 2001; Kaplan et al. 2001; Wolfe et al. 2001; Kaplan and Miller 2003). For example, the large data set of Marsella et al. (2000) contains bimodal age distributions for single glacial features, which are interpreted to represent multiple advances of cold-based ice lobes. There also have been multiple interpretations of cosmogenic nuclide data from southern Baffin Island uplands (e.g., Bierman et al. 2001; Wolfe et al. 2001). And, significant inheritance is found even in scoured bedrock adjacent to Cumberland Sound (Kaplan and Miller 2003). In Labrador, recent cosmogenic nuclide studies have shown that unscoured (weathered) upland areas were covered by the LIS during the LGM (e.g., Clark et al. 2003; Marquette et al. 2004), similar to our findings from the Clyde area (Briner et al. 2003).

Reconstructing Pleistocene ice sheets

There is a growing body of literature that describes highly weathered, "non-glacial" landscapes that have survived cover by ice sheets (e.g., Sugden and Watts 1977; Dyke 1993; Kleman 1994; Bierman et al. 1999; Stroeven et al. 2002; Briner et al. 2003; Hall and Glasser 2003; André 2004; Marquette et al. 2004). Here, we add to this literature by suggesting that the unscoured uplands *and* the unscoured lowlands of the Clyde Foreland were covered by the LIS during the last glacial cycle. The preservation of raised marine shorelines and deltas, and meltwater channels that grade to them, on the Clyde Foreland and adjacent Aston Lowlands (Davis et al. 2002; Coulthard 2003) supports this conclusion. Similar results were recently found on Svalbard, where erosive LGM ice was constrained to fiords and cross-shelf troughs and non-erosive LGM ice preserved pre-LGM beaches and other surficial sediments on adjacent lowlands (Landvik et al. in press).

This study raises several important points regarding the use of CE dating in arctic glacial landscapes. Erratics in terrains covered by cold-based ice may persist beneath subsequent glaciations, creating a complex pattern of exposure ages. In these landscapes, glacial erosion of bedrock surfaces may be insufficient to remove previously accumulated cosmogenic nuclides (Davis et al. 1999), which even has been shown along southern ice-sheet margins (cf. Colgan et al. 2002). Thus, CE ages on both bedrock and erratics in such terrains may provide more information regarding ice-sheet dynamics than chronology.

Land–sea correlations

Marine sediment cores collected from Baffin Bay, adjacent to the Clyde Region, provide an opportunity to compare our terrestrial record with the marine record. Recent findings of major and rapid reorganizations of the LIS periodically throughout the last glaciation (represented by Heinrich Events and Baffin Bay Detrital Carbonate (BBDC) layers; Andrews et al. 1998; Andrews and Barber 2002) may have important implications for fluctuating ice margins on the Clyde Foreland. Andrews et al. (1998) compiled detrital carbonate data from numerous Baffin Bay marine cores. They found evidence for seven detrital carbonate layers, interpreted as ice-rafted debris events, between ~51 and ~12 ka. The BBDC layers are interpreted to represent an increase in ice-sheet calving because of the advection of relatively warm water into Baffin Bay, possibly following Heinrich Events. This scenario suggests that the LIS had fluctuating marine margins in Baffin Bay throughout MIS 3 and 2 (Andrews et al. 1998). Our CE ages, which suggest a dynamic LIS in the Clyde Region throughout the same interval, support the conclusion of Andrews et al. (1998) of a dynamic glacial history in the Baffin Bay region. The most widespread BBDC event ~12 ka overlaps with our estimate for the final deglaciation of the Clyde Foreland.

Conclusions

Detailed glacial geologic mapping and CE ages lead to a revision of the glacial history of the Clyde Foreland. Cosmogenic exposure ages on erratics from the scoured regions of the Clyde Foreland suggest that these areas were covered by the LIS during the LGM and were deglaciated 15 ka at the coast and ~13 ka at the ice-proximal locations. Multiple CE age clusters from erratics in unscoured regions likely represent a fluctuating cold-based ice margin that reached the Clyde Foreland numerous times during the last glaciation (~12–80 ka). Marine reconstructions from adjacent ocean basins provide evidence for fluctuations of the LIS over the same interval. The existence of cold-based, non-erosive ice on distal sections of the foreland and at high elevations stands in contrast to more erosive ice in the fiords and lowlands; this variable pattern indicates a dynamic LIS with sharp contrasts in basal ice conditions.

Cosmogenic exposure dating is complex in landscapes where ice-sheet basal thermal regimes and glacial erosion were spatially and temporally variable. Evidence from the Clyde Foreland suggests glacial overriding with little or no modification of tors, meltwater channels, unconsolidated surficial sediments, and erratics. Only with a large distribution of CE ages can glacial histories be elucidated in regions where ice largely left a pre-LGM landscape unmodified. In such settings, cosmogenic nuclide data may be just as useful for providing information about ice-sheet processes than ice-sheet histories.

Acknowledgments

R. Austin, B. Clarke, R. Coulthard, D. Goldstein, and M. Robinson assisted in the field and laboratory. We thank the Nunavut Research Institute and the people of Clyde River, particularly J. Qillaq and J. Hainnu, for assistance with field logistics. We thank J. Andrews, J. Landvik, Y. Axford, and R. Coulthard for stimulating discussions on the nature of ice-sheet erosion across the Arctic, P. Bierman and J. Larson for laboratory collaboration, and Y. Axford for revising an earlier draft of this manuscript. This work was funded by National Science Foundation grants (OPP-0004455 and OPP-0138010) to GHM and PTD and by graduate student grants to JPB from the University of Colorado, American Alpine Club, and the Geological Society of America. This work was performed under the auspices of the US. Department of Energy by the University of California, Lawrence Livermore National Laboratory under contract number W-7405-Eng-48. We thank P. Bierman and R. Gilbert for strengthening this manuscript with thoughtful reviews.

References

André, M.-F. 2004. The geomorphic impact of glaciers as indicated by tors in North Sweden (Aurivaara, 68°N). Geomorphology, **57**: 403–421.

Andrews, J.T. 1987. The late Wisconsin glaciation and deglaciation of the Laurentide Ice Sheet. *In* North America and adjacent oceans during the last deglaciation. *Edited by* W.F. Ruddiman and H.E. Wright, Jr. Geological Society of America, Boulder, Colo., The Geology of North America, Vol. K-3, pp. 13–37.

Andrews, J.T., and Barber, D.C. 2002. Dansgaard-Oeschger events: is there a signal off the Hudson Strait ice stream? Quaternary Science Reviews, **21**: 443–454.

Andrews, J.T., Clark, P.U., and Stravers, J.A. 1985. The pattern of glacial erosion across the eastern Canadian Arctic. *In* Quaternary environments: Eastern Canadian Arctic, Baffin Bay, and West Greenland. *Edited by* J.T. Andrews. Allen and Unwin, Winchester, Mass., pp. 69–92.

Andrews, J.T., Kirby, M.E., Aksu, A., Barber, D.C., and Meese, D. 1998. Late Quaternary detrital carbonate (DC-) layers in Baffin Bay marine sediments (67°–74°N): Correlation with Heinrich events in the North Atlantic. Quaternary Science Reviews, **17**: 1125–1137.

Balco, G., Stone, J.O., Porter, S.C., and Caffee, M.W. 2002. Cosmogenic-nuclide ages for New England coastal moraines, Martha's Vineyard and Cape Cod, Massachusetts, USA. Quaternary Science Reviews, **21**: 2127–2135.

Bierman, P.R., and Caffee, M. 2001. Slow rates of rock surface erosion and sediment production across the Namib desert and escarpment, southern Africa. American Journal of Science, **301**: 326–358.

Bierman, P.R., Marsella, K.A., Patterson, C., Davis, P.T., and Caffee, M. 1999. Mid-Pleistocene cosmogenic minimum-age limits for pre-Wisconsin glacial surfaces in southwestern Minnesota and southern Baffin Island: a multiple nuclide approach. Geomorphology, **27**: 25–39.

Bierman, P.R., Marsella, K.A., Davis, P.T., and Caffee, M.W. 2001. Response to Discussion by Wolfe et al. on Bierman et al. (Geomorphology 27 (1999) 25–39). Geomorphology, **39**: 255–260.

Birkeland, P.W. 1978. Soil development as an indication of relative age of Quaternary deposits, Baffin Island, N.W.T., Canada: Arctic and Alpine Research, **10**: 733–747.

Boyer, S.J., and Pheasant, D.R. 1974. Delimitation of weathering zones in the fiord area of eastern Baffin Island, Canada. Geological Society of America Bulletin, **85**: 805–810.

Briner, J.P. 2003. The last glaciation of the Clyde region, northeastern Baffin Island, arctic Canada: Cosmogenic isotope constraints on Laurentide Ice Sheet dynamics and chronology. Ph.D. thesis, University of Colorado, Boulder, Colo., 300 p.

Briner, J.P., Miller, G.H., Davis, P.T., Bierman, P.R., and Caffee, M. 2003. Last Glacial Maximum ice sheet dynamics in arctic Canada inferred from young erratics perched on ancient tors. Quaternary Science Reviews, **22**: 437–444.

Clark, P.U., Brook, E.J., Raisbeck, G.M., Yiou, F., and Clark, J. 2003. Cosmogenic ^{10}Be ages of the Saglek moraines, Torngat Mountains, Labrador. Geology, **31**: 617–620.

Colgan, P.M., Bierman, P.R., Mickelson, D.M., and Caffee, M. 2002. Variation in glacial erosion near the southern margin of the Laurentide Ice Sheet, south-central Wisconsin, USA: Implications for cosmogenic dating of glacial terrains. Geological Society of America Bulletin, **114**: 1581–1591.

Coleman, A.P. 1920. Extent and thickness of the Labrador ice sheet. Geological Society of America Bulletin, **31**: 819–828.

Coulthard, R.D. 2003. The glacial and sea level history of the Aston Lowlands, east-central Baffin Island, Nunavut, Canada. M.Sc. thesis, University of Colorado, Boulder, Colo., 123 p.

Dansgaard, W., Johnsen, S.J., Clausen, H.B., Dahl-Jensen, D., Gundestrup, N.S., Hammer, C.U., Hvidberg, C.S., Steffensen, J.P., Sveinbjornsdottir, A.E., Jouzel. J., and Bond, G. 1993. Evidence for general instability of past climate from a 250-kyr ice-core record. Nature (London), **364**: 218–220.

Davis, P.T., Bierman, P.R., Marsella, K.A., Caffee, M.W., and Southon, J.R. 1999. Cosmogenic analysis of glacial terrains in the eastern Canadian Arctic: a test for inherited nuclides and the effectiveness of glacial erosion. Annals of Glaciology, **28**: 181–188.

Davis, P.T., Briner, J.P., Miller, G.H., Coulthard, R.D., Bierman, P.R., and Finkel, R.W. 2002. Huge >54,000 yr old glaciomarine delta on northern Baffin Island overlain by boulders with <20,000 yr old cosmogenic exposure ages: Implications for non-erosive cold-based ice on Baffin Island during the LGM. Geological Society of America, Abstracts with Programs, **34**: A323.

Denton, G., and Hughes, T. (*Editors*). 1981. The last great ice sheets. Wiley and Sons, New York, N.Y., 484 p.

Dyke, A.S. 1979. Glacial and sea level history of southwest Cumberland Peninsula, Baffin Island, N.W.T., Canada. Arctic and Alpine Research, **11**: 179–202.

Dyke, A.S. 1993. Landscapes of cold-centred Late Wisconsinan ice caps, arctic Canada. Progress in Physical Geography, **17**: 223–247.

Dyke, A.S. 1999. Last glacial maximum and deglaciation Devon Island, arctic Canada: Support for an Innuitian Ice Sheet. Quaternary Science Reviews, **18**: 393–420.

Dyke, A.S., and Prest, V.K. 1987. Late Wisconsin and Holocene history of the Laurentide Ice Sheet. Géographie physique et Quaternaire, **41**: 237–263.

Dyke, A.S., Andrews, J.T., Clark, P.U., England, J.H., Miller, G.H., Shaw, J., and Veillette, J.J. 2002. The Laurentide and Innuitian Ice Sheets during the Last Glacial Maximum. Quaternary Science Reviews, **21**: 9–31.

England, J. 1976. Late Quaternary glaciation of the eastern Queen

Elizabeth Islands, N.W.T., Canada, alternative models. Quaternary Research, **6**: 185–202.
England, J. 1996. Glacier dynamics and paleoclimatic change during the last glaciation of eastern Ellesmere Island, Canada. Canadian Journal of Earth Sciences, **33**: 779–799.
England, J. 1998. Support of the Innuitian Ice Sheet in the Canadian High Arctic during the Last Glacial Maximum. Journal of Quaternary Science, **13**: 275–280.
England, J. 1999. Coalescent Greenland and Innuitian ice during the Last Glacial Maximum: Revisiting the Quaternary of the Canadian High Arctic. Quaternary Science Reviews, **18**: 421–456.
Feyling-Hanssen, R.W. 1976. The stratigraphy of the Quaternary Clyde Foreland Formation, Baffin Island, illustrated by the distribution of benthic foraminifera. Boreas, **5**: 77–94.
Flint, R.F. 1943. Growth of North American ice sheet during the Wisconsin age. Bulletin of the Geological Society of America, **54**: 325–362.
Gosse, J.C., and Phillips, F.M. 2001. Terrestrial in situ cosmogenic nuclides: Theory and application. Quaternary Science Reviews, **20**: 1475–1560.
Gosse, J.C., and Stone, J.O. 2001. Terrestrial cosmogenic nuclide methods passing milestones toward paleo-altimetry. Eos (Transactions, American Geophysical Union), 82, 86, 89.
Gosse, J.C., Evenson, E.B., Klein, J., Lawn, B., and Middleton, R. 1995. Precise cosmogenic ^{10}Be measurements in western North America: support for a global Younger Dryas cooling event. Geology, **23**: 877–880.
Hall, A.M., and Glasser, N.F. 2003. Reconstructing the basal thermal regime of an ice stream in a landscape of selective linear erosion: Glen Avon, Cairngorm Mountains, Scotland. Boreas, **32**: 191–207.
Hughes, T.J. 1998. Ice Sheets. Oxford University Press, New York, N.Y., 343 p.
Hughes, T., Denton, G.H., and Grosswald, M.G. 1977. Was there a late-Würm Arctic ice sheet? Nature (London), **266**: 596–602.
Ives, J.D. 1975. Delimitation of surface weathering zones in eastern Baffin Island, northern Labrador and arctic Norway: A discussion. Geological Society of America Bulletin, **86**: 1096–1100.
Ives, J.D. 1978. The maximum extent of the Laurentide Ice Sheet along the east coast of North America during the last glaciation. Arctic, **31**: 24–53.
Jackson, G.D., Blusson, S.L., Crawford, W.J., Davidson, A., Morgan, W.C., Kranck, E.H., Riley, G., and Eade, K.E. 1984. Geology, Clyde River, District of Franklin; Geological Survey of Canada, “A” Series Map, 1582A, scale 1 : 250 000.
Jennings, A.E. 1993. The Quaternary History of Cumberland Sound, southeastern Baffin Island: The marine evidence: Géographie physique et Quaternaire, **47**: 21–42.
Jennings, A.E., Tedesco, K.A., Andrews, J.T., and Kirby, M.E. 1996. Shelf erosion and glacial ice proximity in the Labrador Sea during and after Heinrich events (H-3 or 4 to H-0) as shown by foraminifera. *In* Late Quaternary palaeoceanography of the North Atlantic margins. *Edited by* J.T. Andrews, (W.E.N., Austin,) H.H. Bergsten, and A.E. Jennings. Geological Society (of London), Special Publication 111, pp. 29–49.
Kaplan, M.R., and Miller, G.H. 2003. Early Holocene delevelling and deglaciation of the Cumberland Sound region, Baffin Island, arctic Canada. Geological Society of America Bulletin, **115**: 445–462.
Kaplan, M.R., Pfeffer, W.T., Sassolas, C., and Miller, G.H. 1999. Numerical modeling of the Laurentide Ice Sheet in the Baffin Island region: the role of a Cumberland Sound ice stream. Canadian Journal of Earth Sciences, **36**: 1315–1326.
Kaplan, M.R., Miller, G.H., and Steig, E.J. 2001. Low-gradient outlet glacies (ice streams?) drained the northeastern Laurentide ice sheet. Geology, **29**: 343–346.
Kleman, J. 1994. Preservation of landforms under ice sheets and ice caps. Geomorphology, **9**: 19–32.
Kohl, C.P., and Nishiizumi, K. 1992. Chemical isolation of quartz for measurement of in-situ-produced cosmogenic nuclides. Geochimica et Cosmochimica Acta, **56**: 3583–3587.
Lal, D. 1991. Cosmic ray labeling of erosion surfaces: In-situ nuclide production rates and erosion models. Earth and Planetary Science Letters, **104**: 424–439
Landvik, J.Y., Ingólfsson, Ó., Mienert, J., Lehman, S.J., Solheim, A., Elverhøi, A., and Ottesen, D. In Press. Rethinking Late Weichselian ice sheet dynamics in coastal NW Svalbard. Boreas.
Locke, W.W., III 1979. Etching of hornblende grains in arctic soils: An indicator of relative age and Paleoclimate. Quaternary Research, **11**: 197–212.
Løken, O.H. 1966. Baffin Island refugia older than 54,000 years. Science (Washington, D.C.), **153**: 1378–1380.
Løken, O.H., and Hodgson, D.A. 1971. On the submarine geomorphology along the east coast of Baffin Island. Canadian Journal of Earth Sciences, **8**: 185–195.
Marquette, G.C., Gray, J.T., Gosse, J.C., Courchesne, F., Stockli, L., Macpherson, G., and Finkel, R. 2004. Felsenmeer persistence under non-erosive ice in the Torngat and Kaumajet Mountains, Quebec and Labrador, as determined by soil weathering and cosmogenic nuclide exposure dating. Canadian Journal of Earth Sciences, **41**: 19–38.
Marsella, K.A., Bierman, P.R., Davis, P.T., and Caffee, M.W. 2000. Cosmogenic ^{10}Be and ^{26}Al ages for the last glacial maximum, eastern Baffin Island, arctic Canada. Geological Society of America Bulletin, **112**: 1296–1312.
Miller, G.H. 1976. Anomalous local glacier activity, Baffin Island, Canada: Paleoclimatic implications. Geology, **4**: 502–504.
Miller, G.H., and de Vernal, A. 1992. Will greenhouse warming lead to Northern Hemisphere ice-sheet growth? Nature (London), **355**: 244–246.
Miller, G.H., and Dyke, A.S.1974. Proposed extent of late Wisconsin Laurentide ice on eastern Baffin Island. Geology, **7**: 125–130.
Miller, G.H., Andrews, J.T., Short, S.K. 1977. The last interglacial–glacial cycle, Clyde Foreland, Baffin Island, N. W. T.: Stratigraphy, biostratigraphy, and chronology. Canadian Journal of Earth Sciences, **14**: 2824–2857.
Miller, G.H., Wolfe, A.P., Steig, E.J., Sauer, P.E., Kaplan, M.R., and Briner, J.P. 2002. The Goldilocks dilemma: big ice, little ice, or “just right” ice in the eastern Canadian Arctic. Quaternary Science Reviews, **21**: 33–48.
Mode, W.N. 1980. Quaternary stratigraphy and palynololgy of the Clyde Foreland, Baffin Island, N.W.T., Canada. Ph.D. dissertation, University of Colorado, Boulder, Colo., 219 p.
Owen, L.A., Finkel, R.C., Caffee, M.W., and Gualtieri, L. 2002. Timing of multiple glaciations during the late Quaternary in the Hunza Valley, Karakoram Mountains, northern Pakistan: Defined by cosmogenic radionuclide dating of moraines. Geological Society of America Bulletin, **114**: 593–604.
Paterson, W.S.B. 1994. The physics of glaciers. Elsevier, New York, N.Y., 480 p.
Phillips, F.M., Zreda, M.G., Gosse, J.C., Klein, J., Evenson, E.B., Hall, R.D., Chadwick, O.A., and Sharma, P. 1997. Cosmogenic ^{36}Cl and ^{10}Be ages of Quaternary glacial and fluvial deposits of the Wind River Range, Wyoming: Geological Society of America Bulletin, **109**: 1453–1463.
Smith, J.E. 1965. Outer Clyde-Ayr uplands, field report. Canada Dept. Energy, Mines and Resources, Geographical Branch, 47 p.

Steig, E.J., Wolfe, A.P., and Miller, G.H. 1998. Wisconsinan refugia and the glacial history of eastern Baffin Island, Arctic Canada: Coupled evidence from cosmogenic isotopes and lake sediments. Geology, **26**: 835–838.

Stone, J.O. 2000. Air pressure and cosmogenic isotope production. Journal of Geophysical Research, **105**: 23 753 – 23 759.

Stroeven, A.P., Fabel, D., Hättestrand, C., and Harbor, J. 2002. A relict landscape in the center of Fennoscandian glaciation: cosmogenic radionuclide evidence of tors preserved through multiple glacial cycles. Geomorphology, **44**: 145–154.

Sugden, D.E. 1978. Glacial erosion by the Laurentide ice sheet. Journal of Glaciology, **83**: 367–391.

Sugden, D.E., and Watts, S.H. 1977. Tors, felsenmeer, and glaciation in northern Cumberland Peninsula, Baffin Island. Canadian Journal of Earth Sciences, **14**: 2817–2823.

Svendsen, J.I., Astakhov, V.I., Bolshiyanov, D.,Yu., Demidov, I., Dowdeswell, J.A., Gataullin, V., Hjort, C., Hubberten, H.W., Larsen, E., Mangerud, J., Melles, M., Moller, P., Saarnisto, M., and Siegert, M.J. 1999. Maximum extent of the Eurasian ice sheets in the Barents and Kara Sea region during the Weichselian. Boreas, **28**: 234–242.

Swanson, T.W., and Caffee, M.L. 2001. Determination of ^{36}Cl production rates derived from the well-dated deglaciation surfaces of Whidbey and Fidalgo Islands, Wahsington. Quaternary Research, **56**: 366–382.

Wolfe, A.P., Èchette, B., Richard, P.J.H., Miller, G.H., and Forman, S.L. 2000. Paleoecological assessment of an over 90,000-year sequence from Fog Lake, Baffin Island, arctic Canada. Quaternary Science Reviews, **19**: 1677–1699.

Wolfe, A.P., Steig, E.J., and Kaplan, M.R. 2001. An alternative model for the geomorphic history of pre-Wisconsinan surfaces on eastern Baffin Island: A comment on Bierman et al. (Geomorphology 25 (1999) 25–39). Geomorphology, **39**: 251–254.

Zreda, M., England, J., Phillips, F., Elmore, D., and Sharma, P. 1999. Unblocking of the Nares Strait by Greenland and Ellesmere ice-sheet retreat 10,000 years ago. Nature (London), **398**: 139–142.